Norwegian Centre for Climate Services

Evaluation of downscaled reanalysis and observations for Svalbard

Background report for Climate in Svalbard 2100

NCCS report no. 4/2019

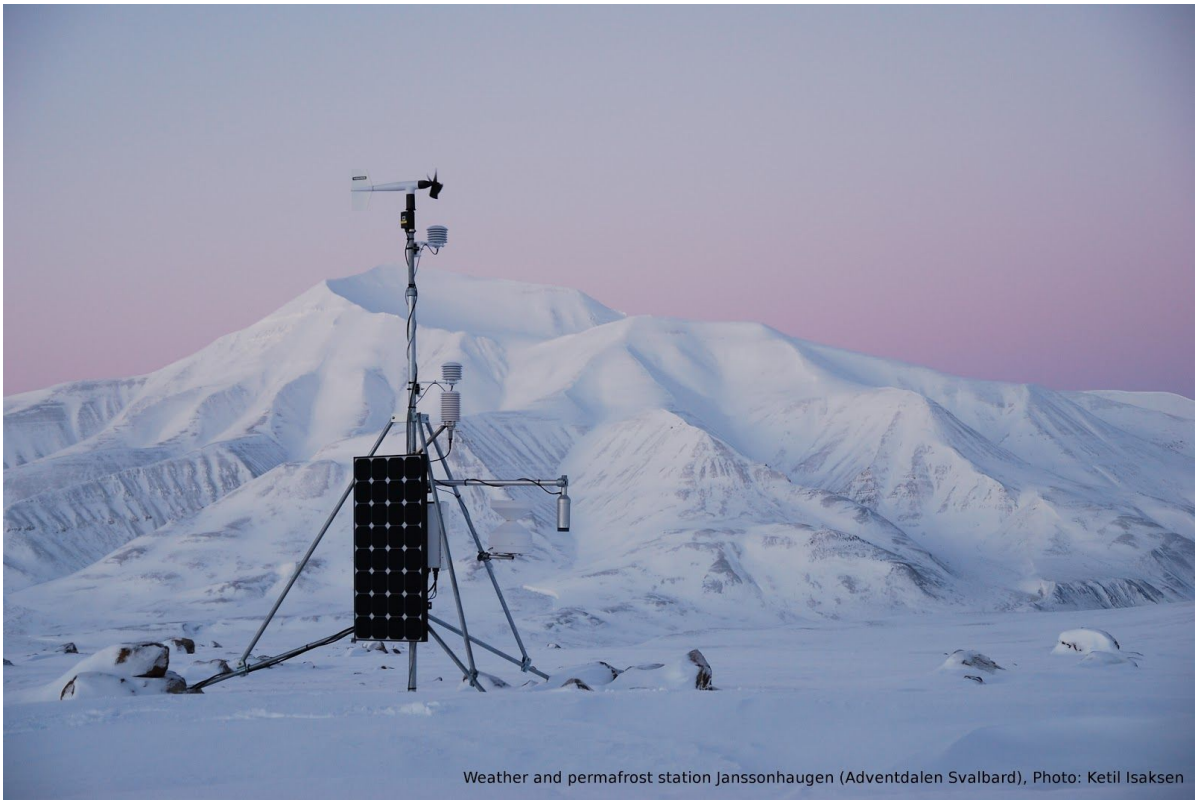

Weather and permafrost station Janssonhaugen (Adventdalen Svalbard), Photo: Ketil Isaksen

Authors
Dagrun Vikhamar-Schuler, Eirik J. Førland, Julia Lutz, Herdis M. Gjelten

The Norwegian Centre for Climate Services (NCCS) is a collaboration between the Norwegian Meteorological Institute, the Norwegian Water Resources and Energy Directorate, the Norwegian Research Centre and the Bjerknes Centre for Climate Research. The main purpose of NCCS is to provide decision makers in Norway with information relevant regarding climate change adaptation. In addition to the partners, the Norwegian Environment Agency is represented on the Board.

The NCCS report series includes reports where one or more authors are affiliated to the Centre, as well as reports initiated by the Centre. All reports in the series have undergone a professional assessment by at least one expert associated with the Centre. Reports in this series may also be included in report series from the institutions to which the authors are affiliated.

Title:	Date
Evaluation of downscaled reanalysis and observations for Svalbard - Background report for Climate in Svalbard 2100	February 2019

ISSN nr.	Report no.
2387-3027	4/2019

Authors	Classification
Dagrun Vikhamar-Schuler[1], Eirik J. Førland[1], Julia Lutz[1], Herdis M. Gjelten[1] [1]: Norwegian Meteorological Institute	Free

Client	Client`s reference

Abstract

In the Norwegian Centre for Climate Service (NCCS) report "Climate in Svalbard 2100", two data sets based on reanalysis were used as supplement to observations in order to describe past and present climate in Svalbard. For temperature and precipitation, the present report provides an evaluation of these two data sets, as well as maps and climate statistics. For both observations and reanalysis the climate statistics include mean values, time series and trends. Various measures are also presented for differences and similarities between values deduced from observations and models. This report may be downloaded from the web portal of NCCS: www.klimaservicesenter.no.

Keywords

Svalbard, climate, reanalysis, observations, analysis, validation, temperature, precipitation

Disciplinary signature

Responsible signature

Contents

1. Introduction

The network of weather stations observing temperature and precipitation in the Svalbard region is sparse. Most of the stations are located on the west coast, and at low altitudes. The biased location and limited number of stations is not sufficient to provide a representative description of temperature and precipitation over the entire Svalbard archipelago. Furthermore, measuring precipitation at Svalbard is a complex challenge; on one hand the precipitation may be overestimated because of contributions from blowing and drifting snow into the gauge. On the other hand, during events with solid precipitation and strong winds, a large part of the precipitation is not "caught" by the gauges (see Sections 4.6 and 4.8). In the harsh Arctic climate, even small re-locations of precipitation gauges may cause severe "homogeneity breaks". Trend studies should be based on homogeneous series, and Section 2.3.2 presents an overview of combination of series (composite series) and homogeneity adjustments performed to establish "homogenised" long-term temperature and precipitation series for the Svalbard region.

Because of the sparse and biased network of weather stations, also reanalysis data was downscaled with the aim of obtaining a more consistent description of temperature and precipitation covering all parts of Svalbard. Two data sets were used:

1. The Sval-Imp data set with 1 km x 1 km spatial resolution which is derived from downscaling the ERA40 and ERA Interim reanalyses.

2. The COSMO climate model simulations with 2.5 km x 2.5 km spatial resolution which are driven with ERA Interim reanalysis data.

Both data sets are described in detail in Chapter 2.

In this report, the two downscaled reanalysis data sets are evaluated against observed temperature and precipitation at weather stations in the region. Aggregated values based on reanalysis are also extracted for entire Svalbard, and for three defined subregions (see Section 2.4). The studies include climatological maps of annual and seasonal mean temperature and precipitation for the "reference period" $1971 - 2000$ and a description of the temperature and precipitation development at selected locations.

The results of this report are used as background for climate analyses and hydrological modelling in the report "Climate in Svalbard 2100" (Hanssen-Bauer et al., 2019).

2. Data and methods

2.1 Sval-Imp data set

For the analysis, we mainly used a downscaled reanalysis data set for Svalbard generated at the University of Oslo (hereafter called the Sval-Imp data set) (Østby et al., 2017; Schuler, 2018). This data set consists of atmospheric variables at the surface level (temperature, precipitation, radiation, etc.) often needed to force terrestrial process models (permafrost, glacier mass balance, seasonal snow, surface energy balance). For the period $1957 - 2017$ ERA40 and ERA-Interim reanalysis data were downscaled using an intermediate complexity model, involving a blend of interpolation techniques and simplified dynamics. The Sval-Imp data set was originally produced for running a mass balance model for glaciers at Svalbard, to study regional and temporal changes. ERA40 covers the period from 1957 to 2002, while ERA-Interim covers the period from 1979 to 2017. The Sval-Imp data set has a spatial resolution of 1 km x 1 km, a temporal resolution of 6 hours, and is freely available for download from Norstore (Schuler, 2018).

2.2 COSMO-CLM data set

To provide a supplementary downscaled reanalysis data set of hourly parameters for the period 2004-2016 (hereafter CCLM data set), the regional climate model COSMO-CLM (Früh et al., 2016) was driven by the ERA-Interim reanalysis over Svalbard at a spatial resolution of 2.5 km x 2.5 km. The CCLM is a non-hydrostatic regional climate model based on the COSMO (Consortium for Small-scale Modeling) numerical weather prediction model (`http://www.cosmo-model.org`). Details on the COSMO-CLM model can be found on the model community's web page `http://www.clm-community.eu/`.

The model set-up for the Svalbard simulations follows the one for the COSMO-CLM simulations covering Europe (Kotlarski et al., 2014). This includes a radiation scheme following Ritter and Geleyn (1992), and a Kessler-type microphysics scheme (Kessler, 1995) with ice-phase processes for cloud water, rain and snow. However,

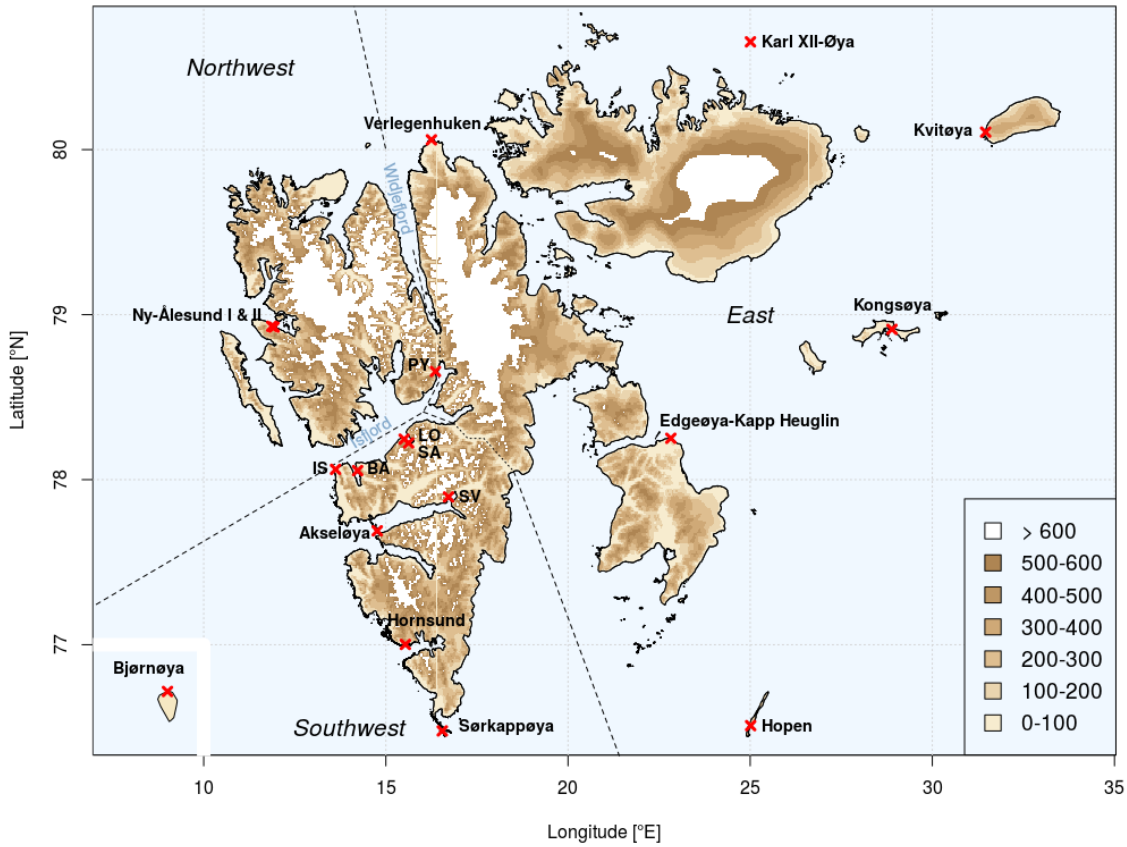

Figure 2.1 – Map of the location of weather stations at Svalbard and the three sub-regions East, Northwest and Southwest. Note that for some stations only the abbreviations from Table 2.1 are used.

due to the high spatial resolution of the current simulation, no convection parametrisation, previously identified as a main reason for biases and uncertainties in climate models (Prein et al., 2015), is needed. Vertically, the model domain consists of 40 atmospheric layers reaching up to 23 km (ca. 40 hPa) and 9 soil layers down to 11.5 m using a multilayer soil model (Schrodin and Heise, 2002). Sea surface temperature and concentration of sea-ice is specified by the driving model, in this case the ERA-Interim reanalysis, which is interpolated to the regional climate model grid and land-sea mask. To account for spin-up, the first six months (July-December 2003) of the simulation have been neglected.

From the CCLM data set, hourly fields of ten surface variables (2 m temperature, relative humidity, rain- and snowfall amount, x- and y-component of 10 m wind, surface and mean sea level pressure, and downward long- and shortwave radiation at the surface) are freely available for download on the Thredds server from the

Meteorological Institute[1].

2.3 Climate series from weather stations

2.3.1 Station network

The network of weather stations observing temperature and precipitation in the Svalbard region is sparse (see Figure 2.1). Most of the stations are located on the west coast, and at low altitudes. In addition, the measuring period for the different variables varies from station to station (see Table 2.1).

St.no	Station name	Start	End	Alt (masl)	Lat	Lon	Type
99710	**BJ**ØRNØYA	1920		16	74.5	19.0	WS
99720	**HO**PEN	1946		6	76.5	25.0	WS
99735	**ED**GEØYA-K.HEUGLIN	2007		14	78.3	22.8	AWS
99740	**KO**NGSØYA	2012		20	78.9	28.9	AWS
99752	**SØ**RKAPPØYA	2010		10	76.5	16.5	AWS
99754	**H**ORN**S**UND	1978		10	77.0	15.5	WS
99760	**SV**EAGRUVA	1978		9	77.9	16.7	WS
99765	**AK**SELØYA	2010		20	77.7	14.8	AWS
99790	**IS**FJORD RADIO	1934		7	78.1	13.6	WS/AWS
99820	**BA**RENTSBURG	1912*		40	78.1	14.2	WS
99840	**S**VALBARD **A**IRPORT	1975		28	78.2	15.5	WS
99860	**LO**NGYEARBYEN	1957	1977	37	78.2	15.6	WS
99880	**PY**RAMIDEN	1948**		20	78.7	16.4	WS/AWS
99900	NY-ÅLESUND I	1969	1974	42	78.9	11.9	WS
99910	NY-ÅLESUND	1974		8	78.9	11.9	WS
99927	**VE**RLEGENHUKEN	2010		8	80.1	16.3	AWS
99935	**KA**RL XII-ØYA	2007		5	80.7	25.0	AWS
99938	**KV**ITØYA	2012		10	80.1	31.5	AWS

Table 2.1 – Metadata for manned (WS) and automatic (AWS) weather stations at Svalbard. Bold letters indicate the abbreviations used in this report.
* Data from Green Harbour 1912-1930, **No measurements for the years 1957-2011

In this report we use observations from stations for temperature and/or precipitation to validate and compare the Sval-Imp and the CCLM data sets. Air temperature is a more robust variable to measure than precipitation, because measuring precipitation under windy conditions is challenging in Arctic regions (see Section 2.3.2).

[1] `http://thredds.met.no/thredds/catalog/metusers/andreasd/SVB_GMB_forcing/ERAInterim_driven_2004-2017/catalog.html`

Figure 2.1 shows a map of the manned and automatic weather stations in the Svalbard region [2]. Also three subregions that were defined for the "Climate in Svalbard 2100" report are marked (see Section 2.4). Table 2.1 provides metadata for the weather stations. Temperature is measured at all stations, while precipitation is measured at the WS stations and a few AWS stations. In the recent years, several new automatic stations were established, e.g. Platåberget at 455 m above sea level. However, these newest stations are not in Table 2.1 since the time series are too short for being used as validation data in this study.

2.3.2 Composite and homogenised historical temperature and precipitation series

To study historical climate variations in the Svalbard region, there is a need for long-term instrumental series. Since the first permanent weather station at Svalbard was established in Green Harbour in 1911, there have been several re-locations of the various weather stations in the region. Because of the harsh climate and large local climate gradients, even small re-locations or instrumental changes at Arctic measuring sites may cause substantial changes (inhomogeneities) in the measuring conditions (Peterson et al., 1998). Regarding precipitation, the gauges are exposed to "undercatch" during events with high winds and solid precipitation, and partly "overcatch" as well because of drifting snow (Førland and Hanssen-Bauer, 2000). Identification of inhomogeneities in Arctic climate series is also hampered by the sparse station network (Figure 2.1). For studies of long term variability and trends, these inhomogeneity breaks must be adjusted because they can have the same order of magnitude as typical long-term climatic trends (Nordli et al., 1996).

A homogenisation analysis of the Norwegian Arctic precipitation series was performed in the mid-1990s using the SNHT method (Nordli et al., 1996). Because of later re-locations of the precipitation gauges at Hopen and Svalbard Airport it has been necessary to conduct new homogenisation analyses for these stations. For this purpose the homogenisation software HOMER (Mestre et al., 2013) was used, and the results are presented below. The precipitation series were tested for each season (winter - DJF, spring - MAM, summer - JJA, autumn - SON).

By combining series, homogenised and partly composite long-term temperature and precipitation series have been established for the key Norwegian weather stations in the Arctic. Below is a brief metadata overview for these stations. More detailed metadata for the Norwegian Arctic stations may be found in Steffensen (1982), Steffensen et al. (1996), Nordli et al. (1996), Førland et al. (1997) and Nordli et al. (2014).

[2]Data from these stations is freely available on eklima.met.no

Bjørnøya

The station was established in 1920 at Tunheim in the northeastern part of the island. In August 1941 the station was destroyed by war actions, but re-established in August 1945. In 1947 the station was moved 7.5 km to Herwigshamna on the northern side of the island. Nordli et al. (1996) found the temperature series to be homogeneous, but the precipitation series had to be adjusted for two homogeneity breaks: one in 1926 connected to the installation of a windshield around the gauge, and one because of the re-location in 1947.

Hopen

The station was established by German soldiers in November 1944 and operated until July 1945. In October 1945 the station was re-established at Hopen Radio. The temperature series was tested and found to be homogeneous (Nordli et al., 1996). The precipitation gauge was re-located in 1997, and a new homogenisation analysis for precipitation was performed in 2018 by use of the Homer software. The homogenised series from Bjørnøya was chosen as the primary reference series. The test results for the winter season, with Bjørnøya as reference station, were not satisfactory, and therefore downscaled reanalysis data (Østby et al., 2017) for Hopen was used as a reference data set for the winter season.

The homogeneity testing revealed a severe homogeneity break after the re-location in 1997 (see Fig. 2.2a). For autumn, winter and spring the adjustment factors were 0.57, 0.41 and 0.49 respectively (see Table 2.2); i.e. the average precipitation measured at the new site are around half the values at the old site. For the summer season the difference is smaller (adjustment factor 0.82). The adjustment factor for annual precipitation was 0.60. The large homogeneity break is probably connected to a combination of strong winds and solid precipitation on Hopen: The new site may be more exposed to wind ("undercatch") and less influenced by drifting snow than the old site. During summer there is no drifting snow, and most of the precipitation is falling as rain. Consequently the undercatch is lower, resulting in a smaller difference in measured precipitation between the two measuring sites. After adjusting the precipitation before 1997 with the factors in Table 2.2, the precipitation series looks homogeneous when compared to Bjørnøya (see Fig. 2.2b, lower part). However, a possible homogeneity break in 1979 is indicated when comparing measured precipitation against reanalysis data (Fig. 2.2b, upper part). This is probably due to an inhomogeneity in the reanalysis, where data from ERA40 and ERAinterim are joined together in 1979 (Section 2.1). It should be pointed out that the recent homogenisation analysis focused on the break in 1997, there may still be other inhomogeneities in the series.

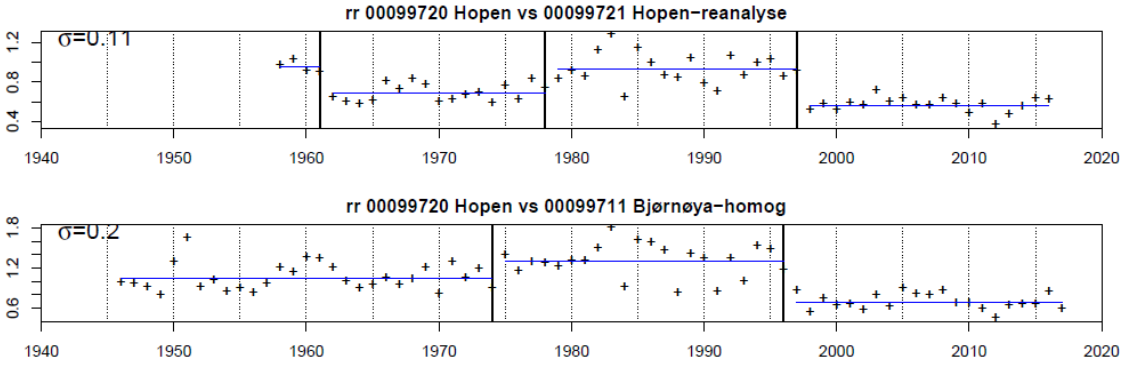

(a)

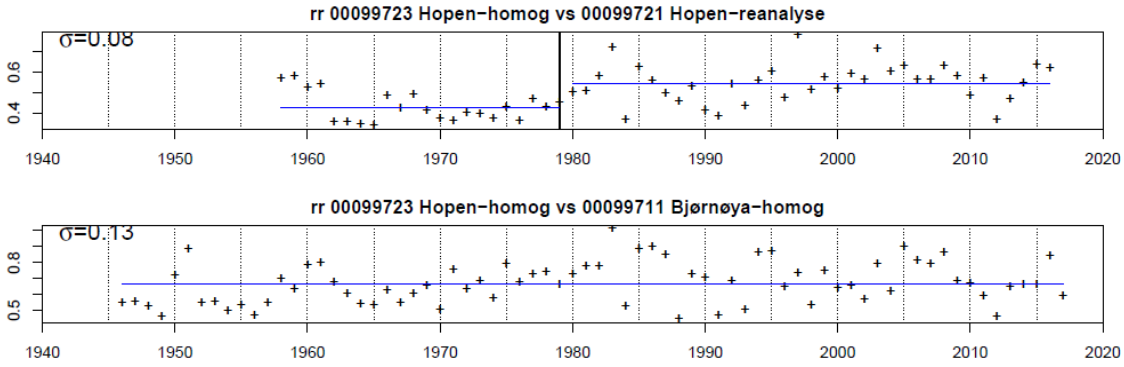

(b)

Figure 2.2 – Relative difference series of annual precipitation between Hopen vs. reference series (Bjørnøya or reanalysis data): a) before adjustment, and b) after adjustment of the break in 1997. The blue line is the mean of the difference series. The black vertical lines indicate homogeneity breaks.

Hornsund

The weather station was established at the Polish research station in Hornsund in 1978. For temperature a composite and homogenised series is established back to 1931 (Gjelten et al., 2016).

Sveagruva

A weather station was established at Sveagruva in 1978 and is still operative. Because of data gaps, re-locations and instrumental changes, the temperature and precipitation series from Sveagruva are not analysed in this report.

Season	Reference series	Adjustment factor
Winter (DJF)	Reanalysis	0.41
Spring (MAM)	Bjørnøya	0.49
Summer (JJA)	Bjørnøya	0.82
Autumn (SON)	Bjørnøya	0.57

Table 2.2 – Adjustment factors for the Hopen precipitation series before homogeneity break in 1997.

Isfjord Radio

The weather station was established in 1934 but was destroyed by war actions in September 1941. The station was re-established at the same site in August 1946, but closed down in June 1976. In 2014 a new automatic weather station was installed. For temperature, the gap between 1976 and 2014 was interpolated partly by use of provisional automatic recordings and partly by regressions to series from Barentsburg and Ny-Ålesund. Thus a continuous daily temperature series is established back to 1934, except for the gap during the Second World War. The temperature series was found to be homogeneous. For precipitation no data exist for the period 1976-2015.

Barentsburg

A Russian weather station was established in Barentsburg in 1933. The station is located only 2.5 km north of Green Harbour, which was the first regular Norwegian weather station in the Arctic. The weather station at Green Harbour was operative from December 1911 to August 1930. More details on metadata and homogeneity for the temperature series from Barentsburg are presented by Nordli et al. (2014).

Svalbard Airport/Longyearbyen

The measurements at the weather station at Svalbard Airport started in August 1975, but some shorter and longer series back to 1911 exist for Longyearbyen. A detailed description of available temperature series for the Longyearbyen area and supplementary observations from hunting and scientific expeditions, is presented by Nordli et al. (2014), who used these series to develop a composite homogenised temperature series for Svalbard Airport back to 1898.

For precipitation no inhomogeneity was found when the precipitation series from Svalbard Airport and Longyearbyen were joined to a composite series back to 1912. However there was a small re-location of the precipitation gauge at the airport in October 2004, and a new homogenisation analysis was performed in 2018. The

homogenised series from Ny-Ålesund (Nordli et al., 1996) was chosen as reference, and the adjustment factors are presented in Table 2.3. By using these adjustment factors the Svalbard Airport precipitation series looks homogeneous when compared to Ny-Ålesund.

Season	Reference series	Adjustment factor
Winter (DJF)	Ny-Ålesund	0.79
Spring (MAM)	Ny-Ålesund	0.84
Summer (JJA)	Ny-Ålesund	0.98
Autumn (SON)	Ny-Ålesund	0.82

Table 2.3 – Adjustment factors for the Svalbard Airport precipitation series before the homogeneity break in 2004.

Ny-Ålesund

During the years 1950−1953 and 1961−1968 irregular measurements were performed by employees of the Kings Bay Kull Kompani and the ESRO telemetry station. A regular weather station was established in 1969. In July 1974 the station was moved from the ESRO station to the telegraph station. The re-location did not influence the homogeneity of the temperature series, but the precipitation series had to be adjusted (Nordli et al., 1996). The series of monthly mean temperatures from Isfjord Radio and Ny-Ålesund were joined to establish a homogenised composite temperature series for Ny-Ålesund back to 1934 (Førland et al., 1997). For the precipitation series only one inhomogeneity was found and adjusted for. This break was induced by the re-location in 1974 which caused increased gauge catch, especially during winter and spring (Førland et al., 1997).

2.4 Comparison of observations and model data

We have divided Svalbard into three subregions (see Figure 2.1: 1. Northwest, 2. East and 3. Southwest). Various climate statistics have been computed for these three regions, as well as for entire Svalbard, see e.g Section 3.2. Time series for the regions based upon the Sval-Imp data set are computed from 1958, as an area-weighted mean of the 1 km x 1 km grid cells within each region. The time series for weather stations were extracted from the Sval-Imp data set at the grid cell covering the geographic location of the individual stations.

For the weather stations we have compared the data from the Sval-Imp and the CCLM data set with observations of daily and monthly temperature and precipitation.

3. Temperature

3.1 Annual and seasonal maps: 1971-2000

The number of weather stations at Svalbard is too low, and too biased (located on the west coast and at low altitudes) to serve as a basis for producing climatological maps for entire Svalbard. Therefore, the Sval-Imp data set (Section 2.1) is applied to give a more spatially consistent picture of the climatology. We have produced annual and seasonal temperature maps for Svalbard, for the period 1971-2000. The maps are shown in Figures 3.1 - 3.3.

Figure 3.2 shows that though the winter temperatures are 10 °C to 20 °C lower than the summer temperatures, spatial temperature variation is rather similar in winter and in summer. The highest temperatures are found in the southern and southwestern parts of the archipelago, while the lowest temperatures occur in mountainous and glacial areas in the north and east. In winter, also coastal areas in the northeast are very cold.

Many factors affect the spatial temperature pattern at Svalbard, the main ones are ocean currents and sea-ice concentration. The warm West Spitsbergen Current flows from south towards the north on the west coast of Spitsbergen. The cold East Spitsbergen Current flows on the east coast, from north of Nordaustlandet towards the south of Edgeøya and southern parts of Spitsbergen, before it turns north on the west coast of Spitsbergen (Hanssen-Bauer et al., 2019). These ocean currents influence the seasonal sea-ice concentration, particularly in winter and spring. In summer and autumn there is little sea-ice and therefore the temperature maps show a more topographical-dependent pattern.

3.2 Seasonal time series for regions: 1958-2017

Seasonal time series were computed for the three subregions and for entire Svalbard, for details see Section 2.4. The plots for each region are shown in Figure 3.4. The seasons are defined as following: winter (DJF: December, January, February), spring (MAM: March, April, May), summer (JJA: June, July, August) and autumn (SON:

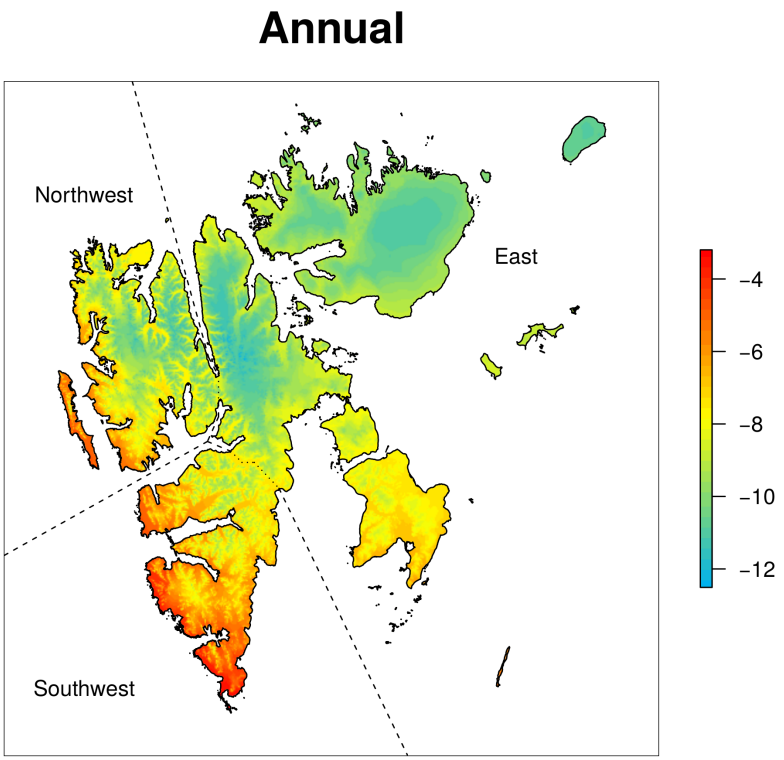

Figure 3.1 – Long-term average of annual temperature in °C (averaged over 1971-2000) from the Sval-Imp data set (see Section 2.1).

September, October, November). The main characteristic for all regions and seasons is increasing temperatures. However, winter temperatures (dark blue coloured lines) increase most rapidly, while summer temperatures (dark green coloured lines) has a slower increase.

3.3 Annual time series for stations and regions

Time series of annual mean temperatures for the weather stations, the subregions and entire Svalbard are shown in Figure 3.5. In this figure, the coloured lines are observations from weather stations, while black and grey colours are computed from the Sval-Imp data set. For the stations Svalbard Airport, Isfjord Radio, Ny-Ålesund, Hornsund and Barentsburg composite observational series were used, see Section 2.3.2.

The time series of annual mean temperatures for the weather stations show a similar long-term pattern. The smoothed graphs indicate that there is variability on multi-decadal scale, leading to mainly positive temperature trends before the 1930s,

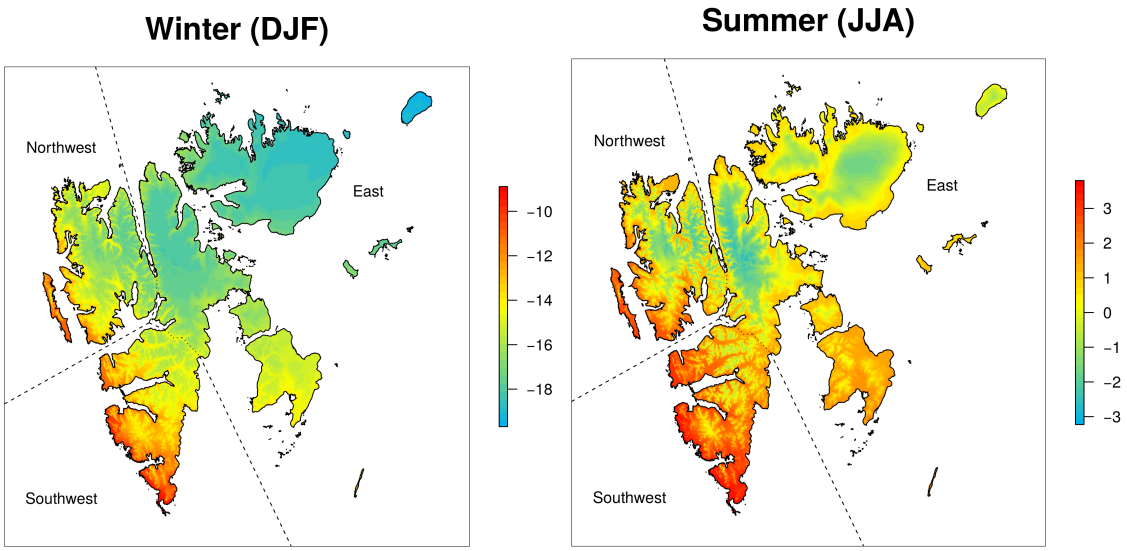

Figure 3.2 – Long-term average of seasonal temperature in °C (averaged over 1971-2000) from the Sval-Imp data set (see Section 2.1). Note that the colour scales are different!

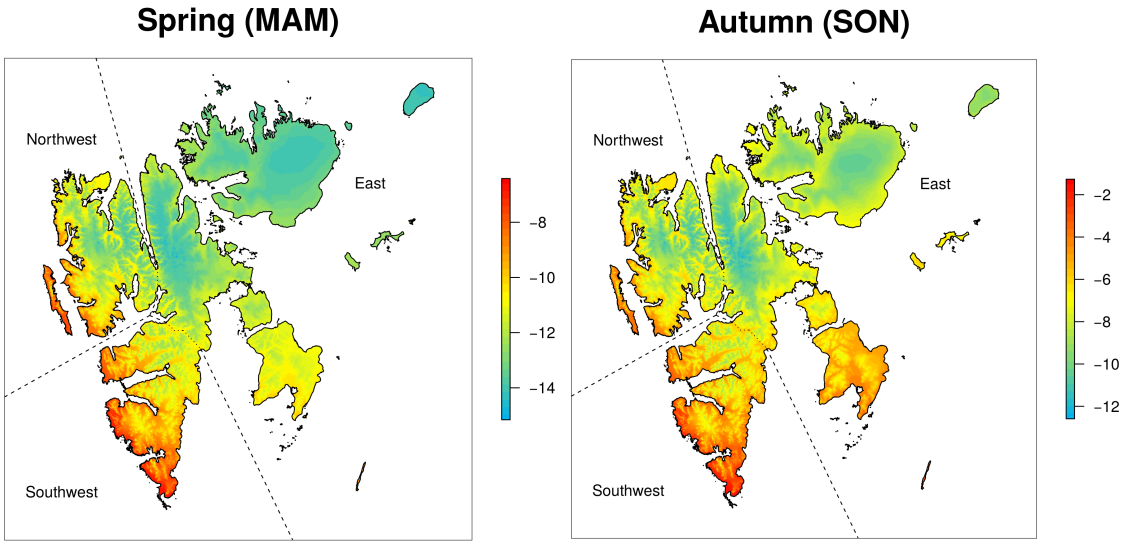

Figure 3.3 – Long-term average of seasonal temperature in °C (averaged over 1971-2000) from the Sval-Imp data set (see Section 2.1). Note that the colour scales are different!

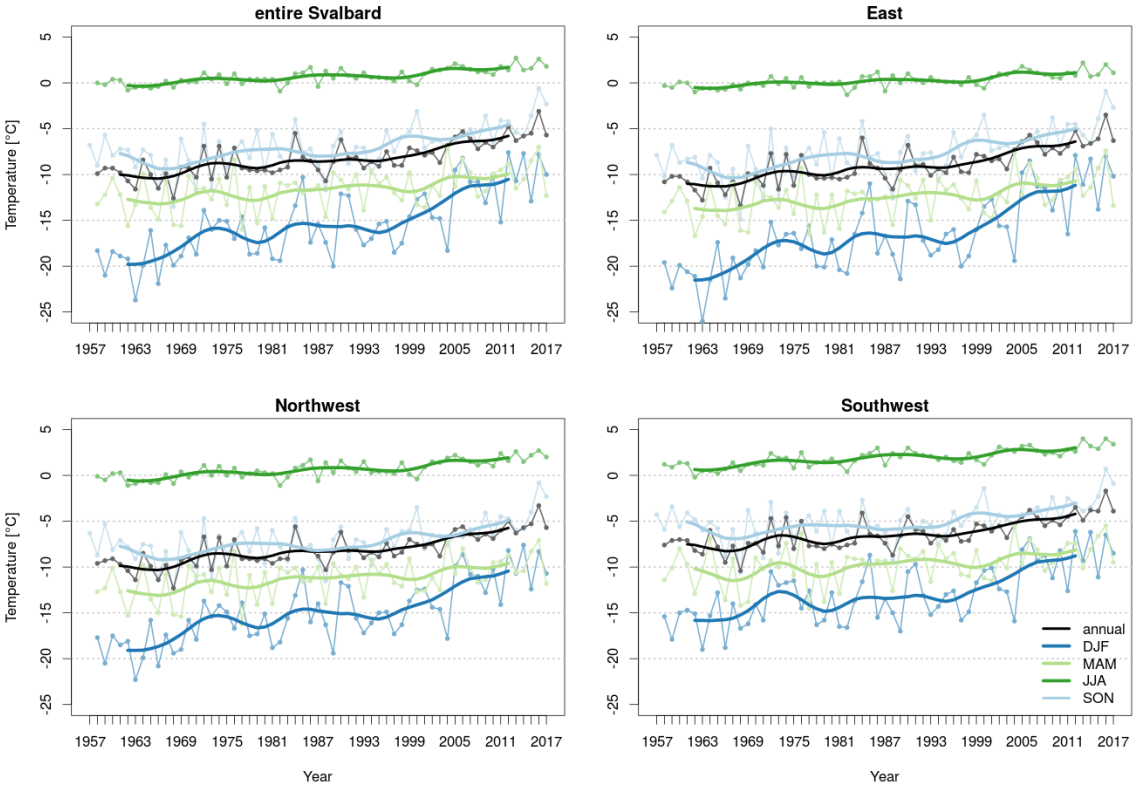

Figure 3.4 – Annual and seasonal mean temperature for entire Svalbard and the three subregions for the years 1958-2017. The connected points indicate the annual values, while the thick continuous curves show the smoothed temperature time series. The smoothed curve was filtered using a Gaussian filter such that variability smaller than 10 years were filtered out.

then a relatively warm period during the subsequent two decades, a temperature decrease from the 1950s to the 1960s, and thereafter a general temperature increase. These features are discussed by Hanssen-Bauer (2002), and can also be seen for other parts of the Arctic (e.g., Polyakov et al., 2003). The warming of the Arctic that started in the 1910s and lasted for two decades is often referred to as the "early 20th century warming", and is one of the most extraordinary climate events of the twentieth century (Bengtsson et al., 2004). The data coverage was limited in the Arctic in the first half of the 20th century, but the spatial pattern of the earlier warm period in the 1930s and 1940s appears to have been different from that of the current warm anomaly. In particular, the current warm period is partly linked to the Northern Annual Mode and affects a broader region (Polyakov et al., 2003).

The regional series show similar trends and decadal patterns as the individual stations. However, they all show lower temperatures than the individual stations,

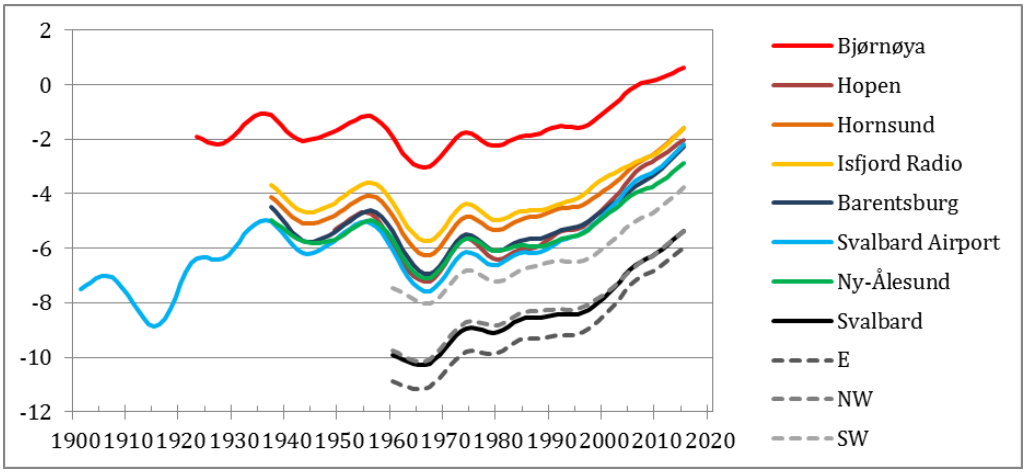

Figure 3.5 – Long-term annual mean temperature in °C. Coloured lines are based on weather station observations, while the black and grey lines are computed from the Sval-Imp data set. All series are smoothed by a Gaussian filter with a standard deviation of three years.

which seems reasonable since the regions cover both higher altitudes and glacier-covered areas. The weather stations are all located near the coast and at low altitudes. The eastern region, which includes Hopen, shows a stronger warming during the latest decades than the other regions.

Figure 3.6 shows smoothed time series extracted from the Sval-Imp data set for temperature at the different stations (see Section 2.4). The station locations are grouped according to their corresponding region. For some stations the observed temperature time series is shown as well. Expectedly, the temperatures in the region Southwest are the highest, whereas the lowest temperatures can be found in the eastern region. As in figure (3.5), the temporal development at all stations is very similar: there is a cooling at the end of the 1950s and the beginning of the 1960s, that is followed by a warming and then again a cooling at the end of the 1970s; afterwards there is a general temperature increase. Especially in the eastern region, the variability among the different curves decreases towards the end of the time series.

The observed temperature at Svalbard Airport is constantly higher than the temperature from the Sval-Imp data set at the corresponding grid point. However, the general pattern is the same for both time series. For Hopen in the east of Svalbard, the temperature from the Sval-Imp data set is higher at the beginning of the time series but the curves meet in the early 1990s. The observed temperature at Ny-Ålesund is much higher than that from the Sval-Imp data set at the beginning of the time series but after 1980 there is good agreement between the observed and the modelled temperature. The reason may be the shift from ERA40 to ERA Interim

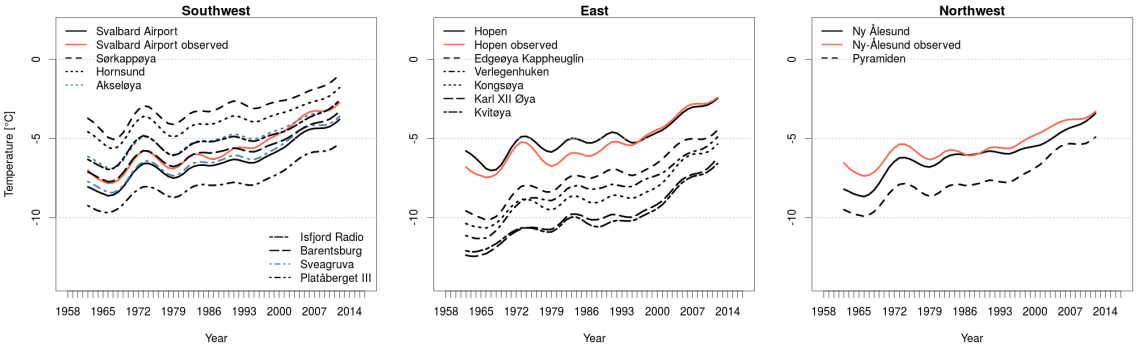

Figure 3.6 – Smoothed mean anual temperature time series for the grid points from Sval-Imp data closest to the actual stations in the three Svalbard subregions for the years 1958 – 2017. Red curves show the smoothed observed temperature time series for certain stations. These curves were filtered using a Gaussian filter such that variabilities smaller than 10 years were filtered out.

in 1978 (see Section 2.1).

3.4 Mean values for 30-year reference periods

Average annual and seasonal temperatures for Svalbard climate stations and regions are shown in Table 3.1. They were computed for the "WMO standard normal period" 1961 – 1990 (left part) as well as for the reference period 1971 – 2000 (right part). The data for the regions is derived from the Sval-Imp data set (see Section 2.4).

	1961 - 1990 average					1971 - 2000 average				
Station name	Ann	DJF	MAM	JJA	SON	Ann	DJF	MAM	JJA	SON
Bjørnøya	-2.3	-7.5	-4.8	3.6	-0.5	-1.7	-6.6	-4.0	3.9	-0.2
Hopen	-6.4	-13.3	-9.9	1.3	-3.7	-5.6	-12.3	-8.8	1.7	-3.1
Hornsund	-5.4	-12.2	-8.8	3.0	-3.6	-4.7	-11.2	-7.7	3.3	-3.2
Isfjord Radio	-5.0	-11.4	-8.6	3.6	-3.6	-4.4	-10.7	-7.7	4.0	-3.1
Barentsburg	-6.1	-13.7	-10.0	3.9	-4.6	-5.5	-12.8	-9.1	4.1	-4.2
Svalbard Airport	-6.7	-15.0	-10.8	4.1	-5.2	-5.9	-13.9	-9.6	4.5	-4.7
Ny-Ålesund	-6.3	-13.7	-9.7	3.5	-5.3	-5.7	-12.9	-8.8	3.7	-4.7
Svalbard total	-9.3	-17.2	-12.4	0.3	-8.1	-8.6	-16.0	-11.8	0.5	-7.4
Svalbard SW	-7.2	-14.3	-10.3	1.4	-7.4	-6.7	-13.4	-9.8	1.8	-5.4
Svalbard NW	-9.1	-16.6	-12.0	0.2	-8.1	-8.4	-15.4	-11.3	0.5	-7.6
Svalbard E	-10.1	-18.6	-13.2	-0.1	-8.8	-9.4	-17.2	-12.7	0.1	-8.1

Table 3.1 – Average annual and seasonal temperature (in °C) for climate stations (from observations) and Svalbard regions (from Sval-Imp data).

The eastern region is coldest in all seasons. This is the region with the highest sea ice concentration, which affects the air temperatures considerably. The difference between summer and winter temperatures is also at maximum in this region. The southwestern region is warmest in all seasons, and the temperature difference between winter and summer is at minimum. The station temperatures are in general higher than the average temperatures for the corresponding regions because they are all situated at low altitudes, and in coastal areas. For stations as well as for regions, both the north-south and the east-west temperature gradient can be seen.

The 1990s were significantly warmer than the 1960s, thus the average annual temperatures over $1971-2000$ are between $0.5\,°C$ and $1\,°C$ higher than the $1961-1990$ values, for regions as well as stations (Table 3.1 and 3.2). Winter temperatures increased considerably more than summer (Table 3.4, left columns), and the difference between winter and summer temperatures has thus decreased slightly.

Station name	1961-1990	1981-2010	1988-2017
Bjørnøya	-0.6	0.5	1.1
Hopen	-0.8	0.8	1.7
Hornsund	-0.7	0.6	1.4
Isfjord Radio	-0.6	0.5	1.2
Barentsburg	-0.6	0.6	1.4
Svalbard Airport	-0.6	0.8	1.7
Ny-Ålesund	-0.6	0.5	1.2
Svalbard total	-0.7	0.7	1.5
Svalbard SW	-0.5	0.6	1.3
Svalbard NW	-0.7	0.6	1.3
Svalbard E	-0.7	0.8	1.6

Table 3.2 – Difference in average annual temperature (in °C) between 1971-2000 and other 30-year periods for weather stations and Svalbard regions. For the stations observed values were used, while the temperatures for the regions were computed from the Sval-Imp data set.

The temperatures have continued to rise after the year 2000 (see Figures 3.4 - 3.6). Temperature differences between the reference period $1971-2000$ and other 30-year periods for regions and climate stations are summarised in Table 3.2. Note that the temperature average for Svalbard for the latest 30 years is $1.7\,°C$ higher than it was during the reference period $1971-2000$.

In addition to the summarising tables (Table 3.1 and 3.2) we have computed aggregated values for the individual months, seasons and annual values for the four periods: $1961-1990$, $1971-2000$, $1981-2010$ and $1988-2017$. The differences between $1971-2000$ and the three other periods were computed as well. These results are presented in the Tables 3.3 and 3.4. Some of the computed values overlap

	Svalbard	East	North-West	Southwest
Annual	-8.7	-9.5	-8.4	-6.7
DJF	-16	-17.2	-15.4	-13.4
MAM	-11.8	-12.7	-11.3	-9.8
JJA	0.5	0.1	0.5	1.8
SON	-7.4	-8.1	-7.6	-5.4
JAN	-16.3	-17.5	-15.5	-13.7
FEB	-16.3	-17.5	-15.7	-13.9
MAR	-14.9	-15.9	-14.4	-12.5
APR	-13.4	-14.4	-12.7	-11.4
MAY	-7.2	-7.8	-6.9	-5.6
JUN	-1.3	-1.5	-1.4	-0.3
JUL	1.7	1.2	1.8	3.1
AUG	1.1	0.6	1	2.6
SEP	-2.3	-2.6	-2.7	-0.8
OCT	-8	-8.6	-8.3	-6
NOV	-12	-13	-11.7	-9.5
DEC	-15.3	-16.5	-14.8	-12.6

Table 3.3 – 30-year reference period (1971 – 2000). Annual, seasonal and monthly mean temperature for subregions and entire Svalbard from the Sval-Imp data set.

	1961-1990 - 1971-2000				1981-2010 - 1971-2000				1988-2017 - 1971-2000			
	Svalbard	East	Northwest	Southwest	Sval	E	NW	SW	Sval	E	NW	SW
Annual	-0.6	-0.7	-0.7	-0.6	0.7	0.8	0.6	0.5	1.5	1.6	1.3	1.2
DJF	-1.2	-1.3	-1.2	-0.9	1.3	1.6	1.2	1	2.8	3.2	2.5	2.3
MAM	-0.6	-0.5	-0.7	-0.5	0.5	0.5	0.4	0.4	1	1.1	0.8	0.8
JJA	-0.2	-0.2	-0.3	-0.4	0.4	0.3	0.3	0.4	0.7	0.6	0.8	0.7
SON	-0.6	-0.7	-0.5	-0.4	0.6	0.8	0.5	0.4	1.4	1.7	1.3	1.2
JAN	-1.3	-1.5	-1.2	-0.9	1.4	1.6	1	1	2.8	3.1	2.3	2.3
FEB	-1.5	-1.5	-1.7	-1.2	1.3	1.5	1.3	1.1	2.6	2.9	2.4	2.2
MAR	-1.9	-2	-2	-1.7	0.1	0.1	0.2	0	0.7	0.7	0.7	0.6
APR	-0.2	-0.2	-0.4	-0.1	0.8	0.9	0.6	0.8	1.5	1.6	1.1	1.4
MAY	0.5	0.5	0.3	0.3	0.5	0.5	0.5	0.4	0.8	0.8	0.7	0.6
JUN	0.1	0.1	0	0	0.2	0.1	0.2	0.3	0.6	0.5	0.7	0.7
JUL	-0.4	-0.3	-0.5	-0.6	0.4	0.4	0.4	0.4	0.7	0.7	0.8	0.7
AUG	-0.4	-0.4	-0.4	-0.6	0.4	0.3	0.4	0.4	0.7	0.6	0.9	0.8
SEP	-0.4	-0.5	-0.3	-0.4	0.2	0.2	0.2	0.2	1.1	1	1.1	1
OCT	-0.2	-0.4	-0.1	0	0.5	0.7	0.3	0.3	1.3	1.4	1.1	1
NOV	-1.2	-1.4	-1.1	-0.9	1.3	1.5	1	0.9	2.1	2.5	1.7	1.7
DEC	-0.8	-1	-0.7	-0.5	1.4	1.6	1.1	1	2.8	3.2	2.3	2.3

Table 3.4 – 30-year reference periods: Difference from 1961 – 1990, 1981 – 2010 and 1988 – 2017 respectively to the reference period 1971 – 2000. Annual, seasonal and monthly mean temperature for subregions and entire Svalbard from the Sval-Imp data set.

with the summarising Tables 3.1 and 3.2. A few characteristics from the monthly reference periods are listed below. Compared to the 1971 − 2000 period:

- March 1961 − 1990 was 1.9 °C colder for the Svalbard region, and the month with the largest temperature increase from 1961 − 1990 to 1971 − 2000.
- June 1961 − 1990 was 0.1 °C warmer for the Svalbard region, and the month with the smallest or no temperature change from 1961 − 1990 to 1971 − 2000.
- December 1988 − 2017 was 2.8 °C warmer for the Svalbard region, and the month with the largest temperature increase from 1971 − 2000 to 1988 − 2017.
- The eastern region has the highest temperature increase among the regions for March, with an increase of 3.2 °C in March.
- May, June, July and August 1988 − 2017 show the smallest temperature increase with 0.5 °C to 0.9 °C increase from the 1971 − 2000 period. All regions show a similar temperature increase for these months.
- The eastern region sticks out as the most temperature-sensitive region from 1971 − 2000 to 1988 − 2017. This region has the strongest temperature increase among the regions in winter (DJF), with 3.2 °C increase, and the smallest increase in summer (JJA) with only 0.6 °C increase.

3.5 Covariation

Figure 3.7 summarises the correlations between observed and modelled temperature (both from the CCLM and the Sval-Imp data set) for the different weather stations locations. To simplify the illustration only R^2 is shown. Note that different time periods were used for the Sval-Imp data and the CCLM model. The correlations are computed using the daily temperature as well as the monthly means, for the whole year but also for the summer (Jun-Jul-Aug-Sep) and winter (Dec-Jan-Feb-Mar) months only. As can be seen, R^2 is very high for almost every station and for both daily and monthly correlations. However, the correlation for the summer months for both methods (CCLM and Sval-Imp) is especially low for Karl XII øya and quite low for Edgeøya (only Sval-Imp), Sørkappøya (only CCLM), Verlegenhuken (only CCLM) and Hopen (only CCLM).

Some examples for these correlations can be found in Fig. 3.8, where scatterplots for the daily observed and the Sval-Imp temperature are shown for four selected stations. One can see that the low temperatures are mostly overestimated by the Sval-Imp data, whereas the temperatures above 0 °C are slightly underestimated. In case of the station Isfjord Radio the correlation between observations and Sval-Imp data is very good.

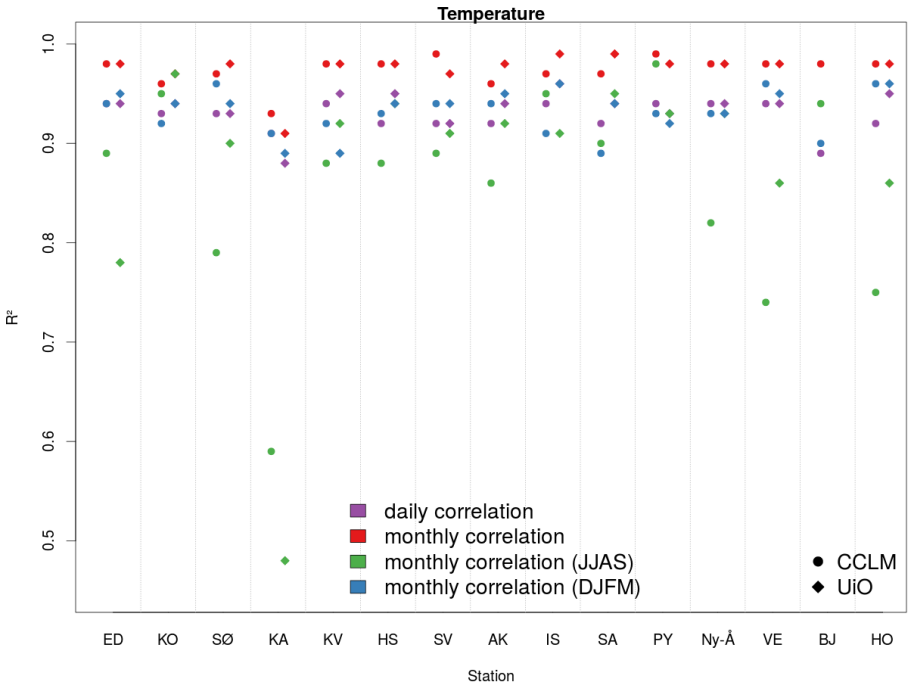

Figure 3.7 – R^2 for the different correlations between temperature from observations, Sval-Imp and CCLM data, respectively. Note that the compared time periods are different for Sval-Imp and CCLM data (the longest possible overlapping period between Sval-Imp or CCLM data and the observations was taken into account). The abbreviations for the station names can be find in Table 2.1.

3.6 Absolute values

Downscaled (Sval-Imp) and observed annual mean temperatures for three selected stations (Table 3.5) indicate a good fit for Hopen and Ny-Ålesund for the three time periods analysed ($1961-1990$, $1971-2000$ and $1988-2017$). The differences between observations and Sval-Imp data at Svalbard Airport in summer and autumn are slightly higher than at Hopen and Ny Ålesund but still in good agreement. However, these three stations are all WMO-stations with easily accessible data, and some (or all) stations are probably assimilated into the reanalysis which serves as a basis for the Sval-Imp data set and thus good correspondence between modelled and observed temperatures is no surprise.

The seasonal mean temperatures (Table 3.5) show that in general the temperatures from the Sval-Imp data set give an underestimate of observed temperatures. The largest discrepancies in the most recent 30-year period ($1988-2017$) are found for summer at Svalbard Airport and Ny-Ålesund (see also Fig. 3.9). On the other hand, the winter temperatures at Hopen and Ny-Ålesund are overestimated in the

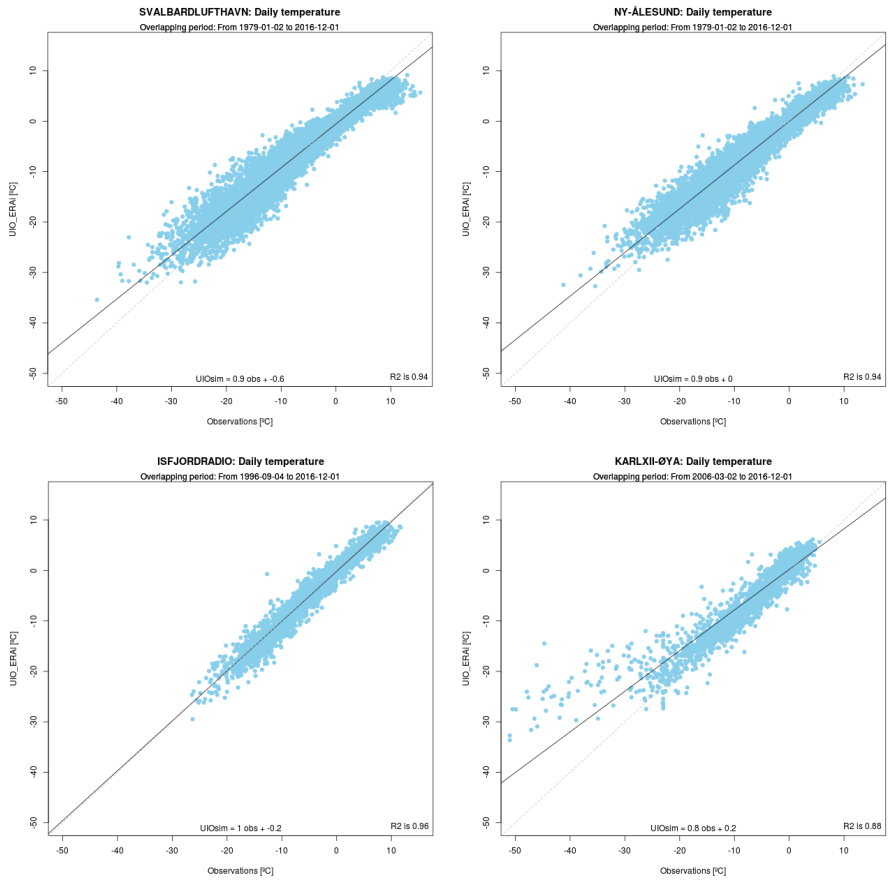

Figure 3.8 – Illustrated examples for Fig. 3.7: Scatterplots for daily temperature from observations and Sval-Imp data for the stations Svalbard Airport (topleft), Ny-Ålesund (topright), Isfjord Radio (bottomleft) and Karl XII øya (bottomright). The lines indicate the regression line between Sval-Imp data and observations.

Sval-Imp data set. For Hopen, Table 3.5 shows that the Sval-Imp data set has a warm bias of 0.2 °C to 0.7 °C for all seasons in the reference period 1971-2000. The annual bias is 0.5 °C. For the period 1988-2017 there was no bias for the annual values between observations and Sval-Imp for Hopen. For the other stations Sval-Imp has for the reference period slightly lower temperatures than observed (Ny-Ålesund: 0.4 °C and Svalbard Airport: 0.8 °C). The biases for the latest 30-years were quite similar to the period 1971-2000. The cold biases are at a maximum in summer, while minor warm biases can be found during winter.

The time development of temperature is illustrated in Table 3.6 as differences between 30-year periods, i.e. $1971-2000$ and $1988-2000$ vs. the standard normal period $1961-1990$. For annual values, Table 3.6 shows changes of 1.8 °C to 2.5 °C

Period	1961-1990			1971-2000			1988-2017		
	OBS	Sval-Imp	Diff	OBS	Sval-Imp	Diff	OBS	Sval-Imp	Diff
ANNUAL									
Hopen	-6.4	-5.7	0.7	-5.6	-5.1	0.5	-3.9	-3.9	0.0
Svalbard Ap	-6.7	-7.4	-0.7	-5.9	-6.7	-0.8	-4.2	-5.2	-1.0
Ny-Ålesund	-6.3	-7.0	-0.7	-5.7	-6.1	-0.4	-4.5	-4.9	-0.4
SPRING									
Hopen	-9.9	-9.2	0.7	-8.8	-8.6	0.2	-7.3	-7.5	-0.2
Svalbard Ap	-10.8	-10.4	0.4	-9.6	-9.8	-0.2	-8.0	-8.7	-0.7
Ny-Ålesund	-9.7	-9.9	-0.2	-8.8	-9.0	-0.2	-7.9	-8.0	-0.1
SUMMER									
Hopen	1.3	2.2	0.9	1.7	2.2	0.5	2.5	2.4	-0.1
Svalbard Ap	4.1	1.5	-2.6	4.5	2.1	-2.4	5.4	3.0	-2.4
Ny-Ålesund	3.5	1.5	-2.0	3.7	2.0	-1.7	4.2	2.6	-1.6
AUTUMN									
Hopen	-3.7	-2.9	0.8	-3.1	-2.6	0.5	-1.6	-1.6	0.0
Svalbard Ap	-5.2	-5.9	-0.7	-4.0	-5.4	-1.4	-3.1	-4.0	-0.9
Ny-Ålesund	-5.3	-5.6	-0.3	-4.7	-5.0	-0.3	-3.7	-4.0	-0.3
WINTER									
Hopen	-13.4	-12.9	0.5	-12.4	-11.7	0.7	-9.6	-9.0	0.6
Svalbard Ap	-15.0	-14.8	0.2	-14.0	-13.7	0.3	-11.2	-11.2	0.0
Ny-Ålesund	-13.7	-14.2	-0.5	-13.0	-12.6	0.4	-10.8	-10.3	0.5

Table 3.5 – Seasonal and annual mean temperatures (in °C) from observations (OBS) and the Sval-Imp data set (Sval-Imp).

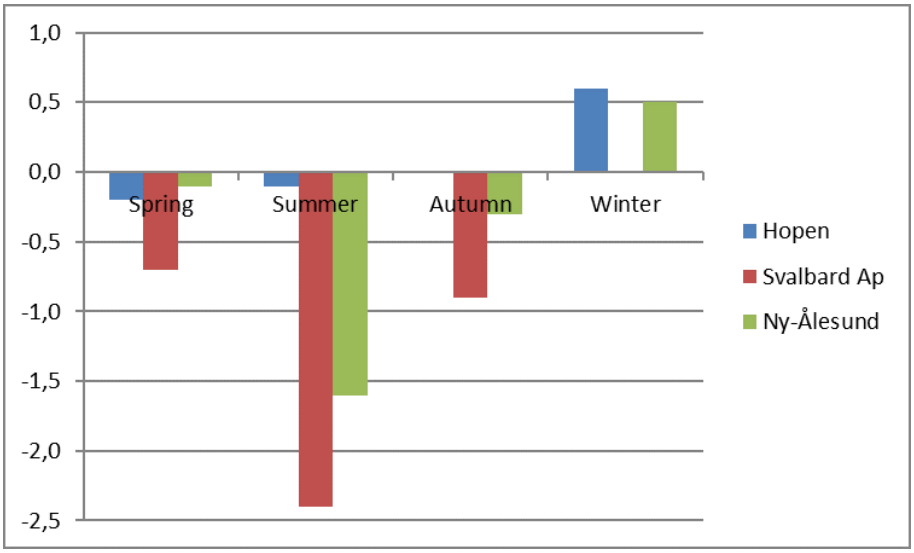

Figure 3.9 – Difference (in °C) between the modelled (Sval-Imp data set) and observed mean temperatures during 1988 – 2017.

Period	1971-2000 vs. 1961-1990			1988-2017 vs. 1961-1990		
	OBS	Sval-Imp	SvalImp-OBS	OBS	Sval-Imp	SvalImp-OBS
ANNUAL						
Hopen	0.8	0.6	-0.2	2.5	1.8	-0.7
Svalbard Ap	0.8	0.7	-0.1	2.5	2.2	-0.3
Ny-Ålesund	0.6	0.9	0.3	1.8	2.1	0.3
SPRING						
Hopen	1.1	0.6	-0.5	2.6	1.7	-0.9
Svalbard Ap	1.2	0.6	-0.6	2.8	1.7	-1.1
Ny-Ålesund	0.9	0.9	0.0	1.8	1.9	0.1
SUMMER						
Hopen	0.4	0.0	-0.4	1.2	0.2	-1.0
Svalbard Ap	0.4	0.6	0.2	1.3	1.5	0.2
Ny-Ålesund	0.2	0.5	0.3	0.7	1.1	0.4
AUTUMN						
Hopen	0.6	0.3	-0.3	2.1	1.3	-0.8
Svalbard Ap	1.2	0.5	-0.7	2.1	1.9	-0.2
Ny-Ålesund	0.6	0.6	0.0	1.6	1.6	0.0
WINTER						
Hopen	1.0	1.2	0.2	3.8	3.9	0.1
Svalbard Ap	1.0	1.1	0.1	3.8	3.6	-0.2
Ny-Ålesund	0.7	1.6	0.9	2.9	3.9	1.0

Table 3.6 – Differences in changes in mean temperature (in °C) between 30-year periods based on observations (OBS) and Sval-Imp data (Sval-Imp). The column SvalImp-OBS shows the differences between changes in the Sval-Imp data set and the observations.

between the period $1961-1990$ and the recent period $1988-2017$. Except for Hopen the differences in changes between observations and Sval-Imp data are within 0.3 °C.

The seasonal changes from $1961-1990$ to $1988-2017$ (Figure 3.10) show that for observations as well as the Sval-Imp data, the largest changes (i.e. warming) are found for the winter season, and the smallest for the summer season. Figure 3.11 indicates that for the winter season, the Sval-Imp data set overestimates the warming at two of the three stations. However, for the island station Hopen, the Sval-Imp data shows a weaker warming than observed for the other seasons.

The main conclusion is that the Sval-Imp data set gives a realistic picture of the temperature conditions in the Svalbard area, though the differences between the summer and winter seasons may be underestimated.

3.7 Seasonal and monthly differences

To compare the Sval-Imp data and the CCLM simulations with the observations for single months and seasons, mean annual cycles were computed for manned as well as automatic weather stations (Table 2.1). To summarise the results, Figure 3.12 shows the absolute biases between the mean annual cycles from the Sval-Imp data, the CCLM model respectively and the observations. The biases for the single months

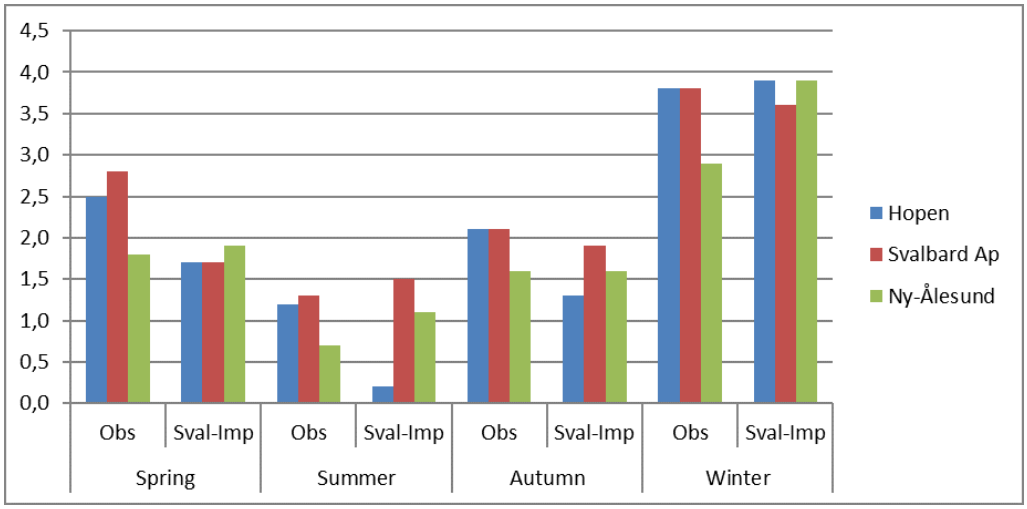

Figure 3.10 – Difference (in °C) in changes from 1961 – 1990 to 1988 – 2017 based on the Sval-Imp data set (Sval-Imp) and observations (OBS).

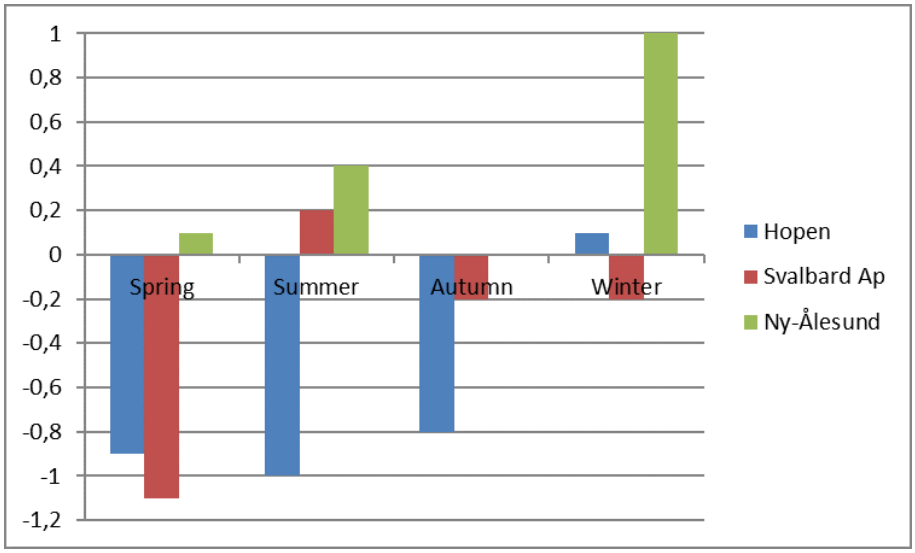

Figure 3.11 – Seasonal differences (Sval-Imp minus OBS) for temperature changes (in °C) from 1961 – 1990 to 1988 – 2017 based on observations resp. the Sval-Imp data set (cf. Table 3.6).

were averaged over the whole year and over the four seasons to illustrate the differences.

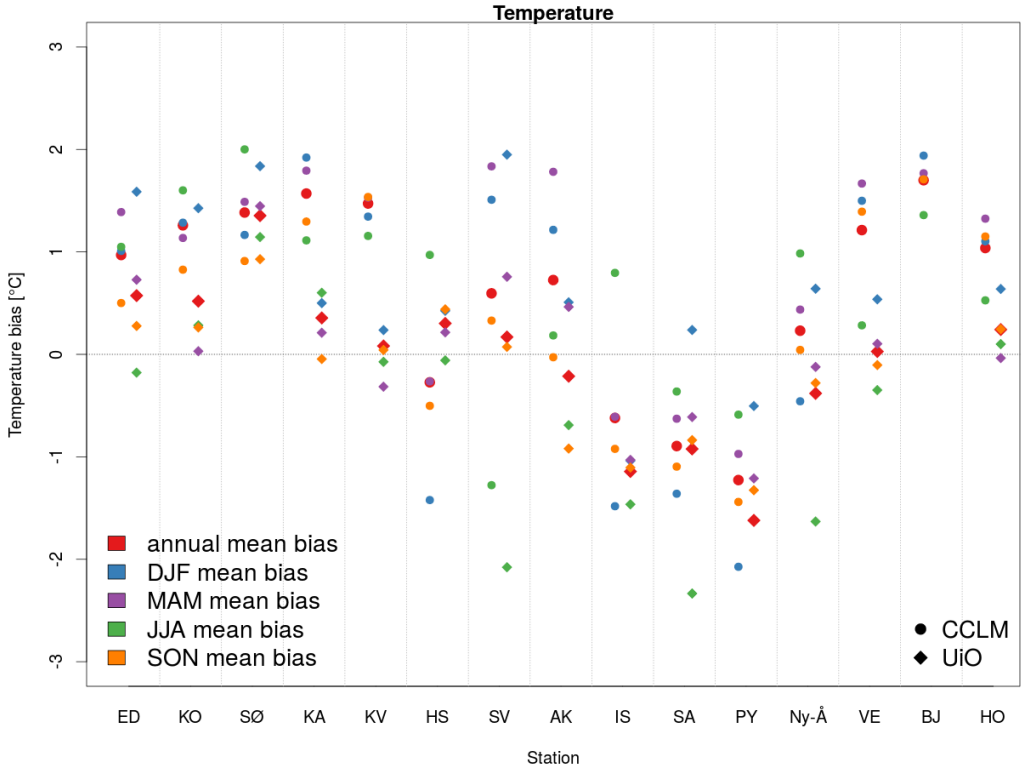

Figure 3.12 – Bias for the mean annual cycle of temperature from CCLM simulations, Sval-Imp data and observations. For the annual bias all twelve months are considered, for the seasonal biases only the corresponding months are taken into account. The abbreviations for the station names can be found in Table 2.1.

In most cases the temperature is overestimated by the models. This applies especially to the eastern stations Edgeøya, Kongsøya, Karl XII Øya, Kvitøya, Verlegenhuken and Hopen. For some stations (Isfjord Radio, Svalbard Airport and Pyramiden) both methods underestimate the temperature except for single seasons. Both methods agree at least in the tendency in the afore mentioned cases. However, in the case of Hornsund the temperature is mainly overestimated by the Sval-Imp data set while it is mainly underestimated by CCLM.

Figure 3.13 shows the mean annual cycle for the Sval-Imp data set (black) and the observations (red) for Hopen and Svalbard Airport. As mentioned above the Sval-Imp data slightly overestimates the observed temperature, especially in winter (Dec, Jan and Feb). This can be seen in Fig. 3.12 as well, where the blue diamond has a higher value as the other diamonds in the column for Hopen. However, the bias is very small and therefore we can conclude that the temperature is very good

represented by the Sval-Imp data set for Hopen. In case of Svalbard Airport, the Sval-Imp method mainly underestimates the observed temperature, especially in summer (Jun, Jul and Aug). This is shown in Fig. 3.12 as well, the green diamond is much lower as the other diamonds in the corresponding column. This time the actual value is much higher though.

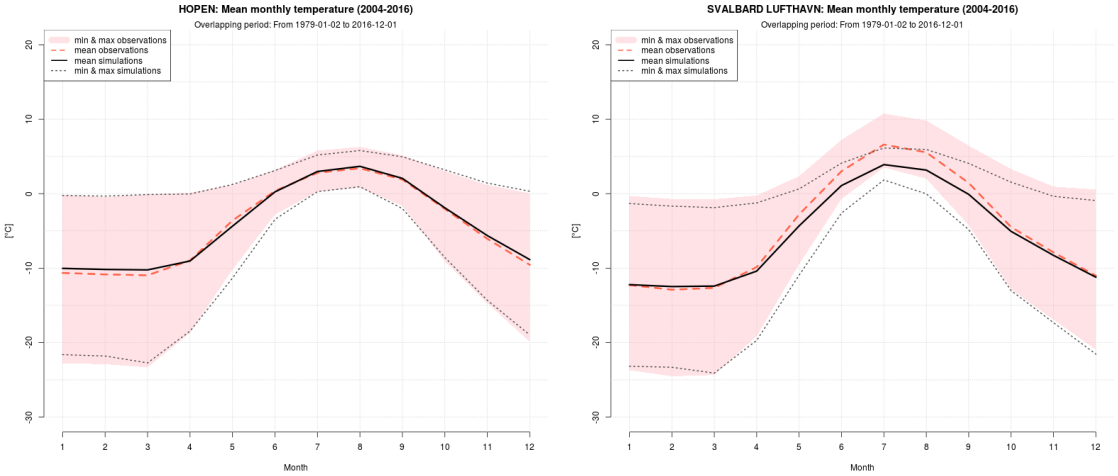

(a) Hopen **(b)** Svalbard Airport

Figure 3.13 – Examples of annual temperature cycles at Hopen and Svalbard Airport: Monthly mean, minimum and maximum temperature from the Sval-Imp data (black) and the observations (red).

3.8 Linear trends

Linear trends are used to quantify the temperature development in Svalbard (Table 3.7), even though there is certain scepticism against using linear trends as a measure for climate change, because such changes not necessarily occur linearly (e.g., Benestad, 2003). Earlier studies (e.g., ACIA, 2005; Førland et al., 2011) have shown that the longest Arctic temperature series can be divided into three periods where the first and the last show statistically significant warming ("early 20th century warming" and the present period of warming), while the middle period shows statistically significant cooling (see also Section 3.2). In the this report we present the trends only for the optimal series (with starting year as the start of the observation period or composite series for the individual weather station), and for the period 1971 to present. The last period is chosen because 1971 is the first year of the reference period in this study.

Station name	Optimal time series (start – 2017) Ann	DJF	MAM	JJA	SON	1971 – 2017 Ann	DJF	MAM	JJA	SON
Bjørnøya (start 1920)	**0.17**	0.15	**0.32**	**0.10**	**0.13**	**0.64**	**1.04**	**0.52**	**0.29**	**0.74**
Hopen (start 1946)	**0.47**	**0.76**	**0.53**	**0.25**	**0.38**	**0.99**	**1.76**	**0.86**	**0.36**	**1.02**
Hornsund (start 1935)	**0.29**	**0.39**	**0.45**	**0.15**	**0.18**	**0.81**	**1.45**	**0.69**	**0.29**	**0.86**
Isfjord Radio (start 1935)	**0.23**	0.24	**0.38**	**0.16**	**0.17**	**0.71**	**1.21**	**0.68**	**0.27**	**0.72**
Barentsburg (start 1934)	**0.26**	0.32	**0.41**	**0.16**	0.16	**0.81**	**1.40**	**0.78**	**0.33**	**0.76**
Svalbard Airport (start 1899)	**0.31**	**0.41**	**0.43**	**0.13**	**0.31**	**1.01**	**1.67**	**0.95**	**0.47**	**1.01**
Ny-Ålesund (start 1935)	**0.24**	0.26	**0.36**	**0.14**	**0.21**	**0.71**	**1.35**	**0.57**	**0.24**	**0.74**
Regions (start 1958)	Optimal time series (1958 – 2017) Ann	DJF	MAM	JJA	SON	1971 – 2017 Ann	DJF	MAM	JJA	SON
Svalbard total	**0.81**	**1.61**	**0.54**	**0.35**	**0.90**	**0.87**	**1.58**	**0.57**	**0.35**	**1.01**
Svalbard SW	**0.67**	**1.25**	**0.47**	**0.42**	**0.78**	**0.75**	**1.27**	**0.51**	**0.39**	**0.84**
Svalbard NW	**0.78**	**1.47**	**0.56**	**0.43**	**0.57**	**0.80**	**1.38**	**0.51**	**0.42**	**0.91**
Svalbard E	**0.88**	**1.79**	**0.55**	**0.30**	**0.67**	**0.95**	**1.78**	**0.61**	**0.31**	**1.11**

Table 3.7 – Linear trends in temperature [°C/decade]. Trends for stations are derived based on weather station observations (Bjørnøya, Hopen) and monthly composite series (Svalbard Airport, Isfjord Radio, Ny-Ålesund, Hornsund, Barentsburg). Trends for regions are derived from the Sval-Imp data set. Bold: Significant trends (5 % level)

Monthly composite series are used for the stations Svalbard Airport, Isfjord Radio, Ny-Ålesund, Hornsund and Barentsburg (see Section 2.3.2). These composite series start much earlier than the starting year described in Table 2.1, because they include some observations from other sites, e.g. to fill missing data. An example is the Svalbard Airport composite series starting in 1898 (Nordli et al., 2014), while the measurements at the airport commenced in 1975.

The trends for the optimal series (Table 3.7, left part) show that the annual mean temperature has increased significantly in the Svalbard Airport/Longyearbyen area from 1899 to present. The linear trend indicates an increase in mean annual temperature of about 3.5 °C during the latest 118 years, which is at least three times the estimated global warming (HadCRUT4) during the same period. The trend is statistically significant (5 % level) in all seasons. Also the other stations show statistically significant positive trends in annual temperatures for the optimal series. For the series starting in the warm period in the 1930s, this is new compared to earlier studies. The temperature has increased in all seasons – with strongest

increase in winter and/or spring.

For the period $1971 - 2017$ trends are calculated for all weather stations as well as for the regions defined above. Regional values are computed using the Sval-Imp data set (Section 2.1). The linear trends (Table 3.7, right part), indicate that during this 47-year period, the annual temperature at all stations and regions has increased by between 3 °C and 5 °C. The average for Svalbard is 4 °C. During this period, the temperature increase was largest in winter, where it adds up to 5 °C - 8 °C for all stations and regions. All seasonal and annual temperature trends are statistically significant at the 5 % level during this period.

These results (Table 3.7, right part) show that the linear trends from the Sval-Imp data are in line with the linear trends from the observations. There are of course differences, but the overall agreement shows that the Sval-Imp data represents a very useful supplement to observations for getting information about trends of the entire Svalbard region. Among the regions and the seasons, the eastern region of Svalbard has the highest temperature trend in winter (1.78 °C per decade), and the lowest trend in summer (0.31 °C per decade).

4. Precipitation

4.1 Annual and seasonal maps: 1971-2000

Maps of annual and seasonal precipitation for Svalbard for the period $1971 - 2000$ are shown in Figures 4.1 - 4.3. The maps were produced based on the downscaled precipitation of the Sval-Imp data set, described in Section 2.1.

The number of weather stations observing precipitation at Svalbard is too low (even lower than the number of stations observing temperature), and too biased (located on the west coast at low altitudes) to serve as basis for producing climatological maps. Therefore, the Sval-Imp data set is applied to give a more spatially consistent picture of the precipitation climatology.

The maps of annual and seasonal precipitation (Figures 4.1 - 4.3) demonstrate highest amounts of precipitation in western mountain areas and lowest values in sheltered valleys and at low elevations in central and northeastern areas.

The annual precipitation at Svalbard Airport is lower than the driest areas on the Norwegian mainland, and also the daily intensities are usually rather low: daily precipitation of 1 mm or more occurs in average just 50 days per year and exceeds 5 mm just 8 days per year (Isaksen et al., 2017). The precipitation frequencies are quite similar for all seasons, except for lower values during spring (MAM). However, despite the rather low frequencies of daily precipitation exceeding 5 mm per day, events with daily rainfall of 25 mm to 50 mm are not uncommon (Dobler et al., 2019).

4.2 Seasonal time series for regions: 1958-2017

Seasonal time series of modelled precipitation for the three subregions (East, Northwest and Southwest) and entire Svalbard are presented in Figure 4.4. The series are computed as described in Section 2.4 for the seasons winter (DJF: December, January, February), spring (MAM: March, April, May), summer (JJA: June, July, August) and autumn (SON: September, October, November).

The precipitation amount for all regions is very similar, the autumn precipitation

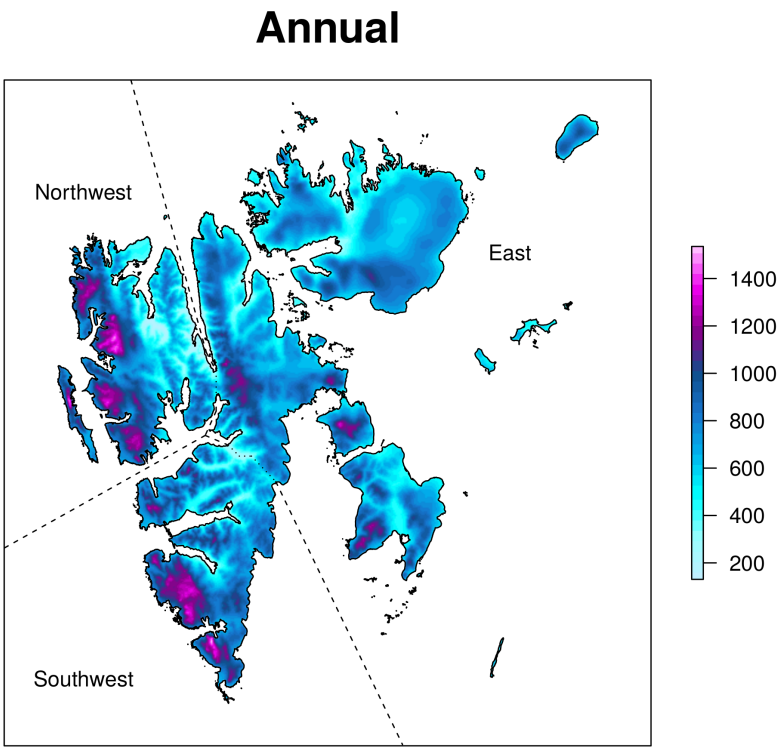

Figure 4.1 – Average annual precipitation (1971 – 2000) in mm from the Sval-Imp data set.

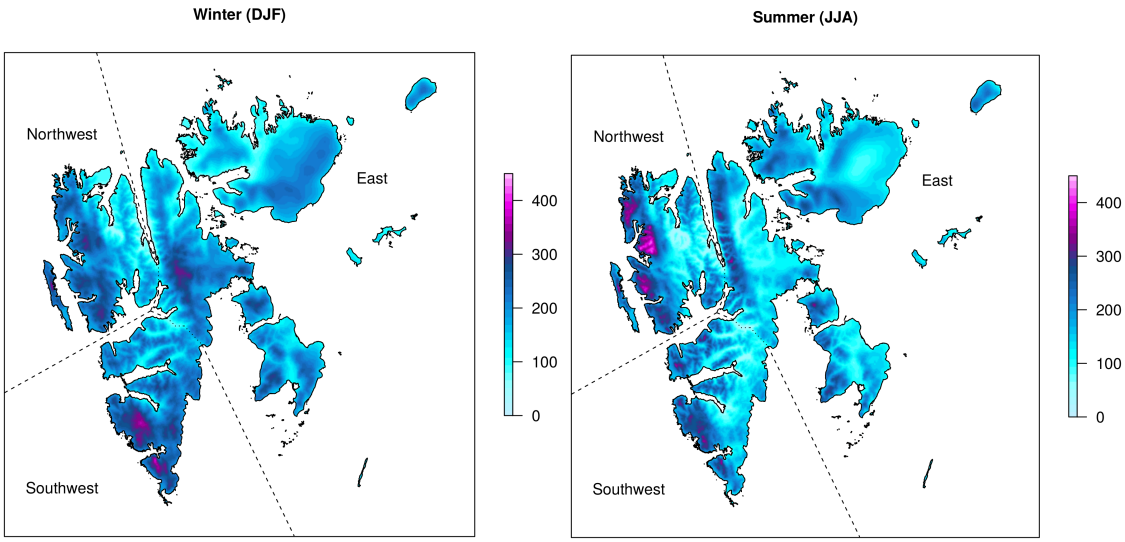

Figure 4.2 – Average winter and summer precipitation (1971 – 2000) in mm from the Sval-Imp data set.

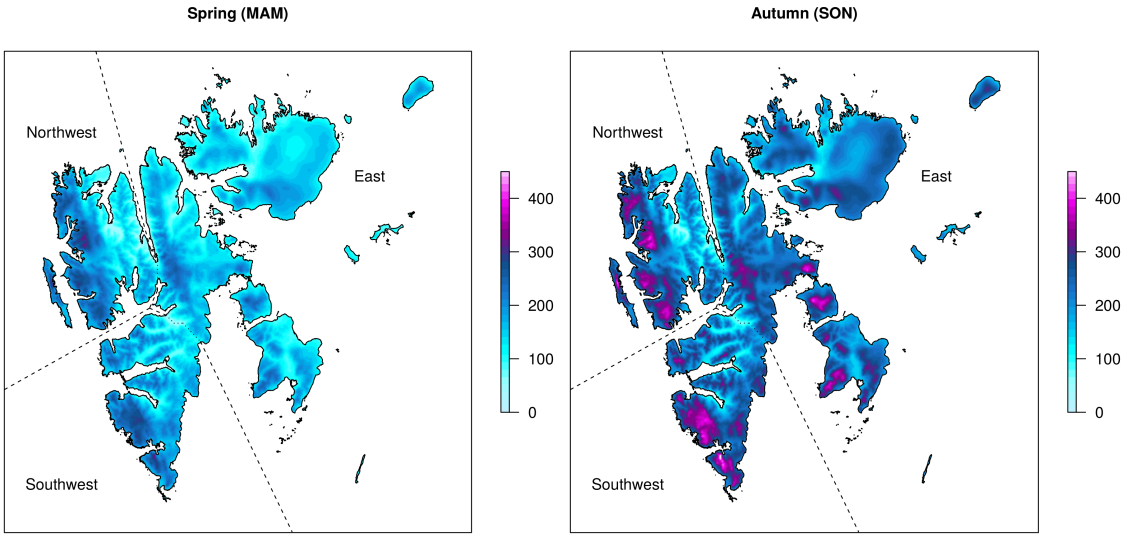

Figure 4.3 – Average spring and autumn precipitation (1971 – 2000) in mm from the Sval-Imp data set.

being the highest for all regions and either the spring or the summer precipitation being the lowest. Except for the autumn precipitation, all the regions and the other seasons show a main characteristic: there is a secondary maximum during the early 1970s. Most of the curves show a further secondary maximum during the early 1990s and a precipitation increase towards the end of the time period.

4.3 Annual time series for stations and regions

In situ precipitation observations from the Arctic are sparse and are subject to many site and gauge issues (e.g. undercatch, reporting of trace precipitation, station/instrumental shifts, changes in measurement protocols, automation), while atmospheric reanalyses often contain wet biases linked to inadequate representation of sea ice as well as inhomogeneities from changes in data streams over time (SWIPA, 2017). For the Norwegian Arctic, a composite, homogenised precipitation series is established for Svalbard Airport back to 1912 (Section 2.3.2). This is one of the longest precipitation series from the Arctic. Also the long-term series from Bjørnøya (1920-present), Hopen (1946-present) and Ny-Ålesund (1968-present) are adjusted for inhomogeneities (see Section 2.3.2).

Figure 4.5 shows long-term variability on a decadal time scale. The coloured curves are based on homogenised observational series from weather stations, while the black and grey curves are computed from the Sval-Imp data set. In contrast to

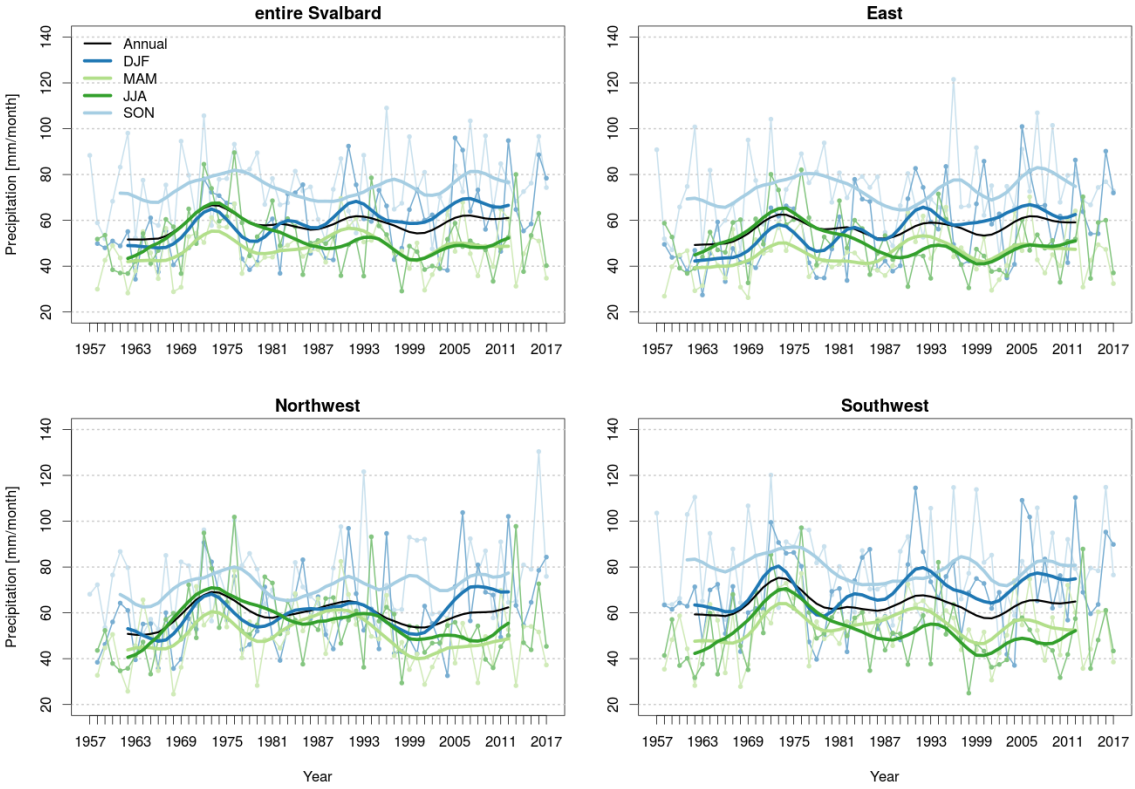

Figure 4.4 – Annual and seasonal precipitation (mm/month) for entire Svalbard and the three subregions for the years 1958 – 2017 from the Sval-Imp data set. The connected points indicate the annual values, while the thick continuous curves indicate the smoothed precipitation time series. The smoothed curves were filtered using a Gaussian filter such that variability smaller than 10 years were filtered out. Note that only the smoothed curve is shown for the annual precipitation.

temperature (Fig. 3.5), the precipitation series show quite different individual long-term patterns. The main reason is that precipitation varies locally on a smaller spatial scale than air temperature. However, most series have some common features: Secondary maxima in the warm periods in the 1930s and 1950s (cf. Fig. 3.5) and secondary minima in the cold periods in the 1940s and 1960s. Unlike most of the observational series (except Barentsburg), the Sval-Imp data series indicates a maximum in the 1970s. Most series show increasing precipitation in the warming period after the year 2000. Hanssen-Bauer and Førland (1998) showed that the precipitation trend at Svalbard Airport from 1912 to the 1990s could be explained to a large degree by variations in the atmospheric circulation in the same period.

Smoothed model-based time series for annual precipitation at the different stations are shown in Fig. 4.6, the stations are grouped according to their corresponding

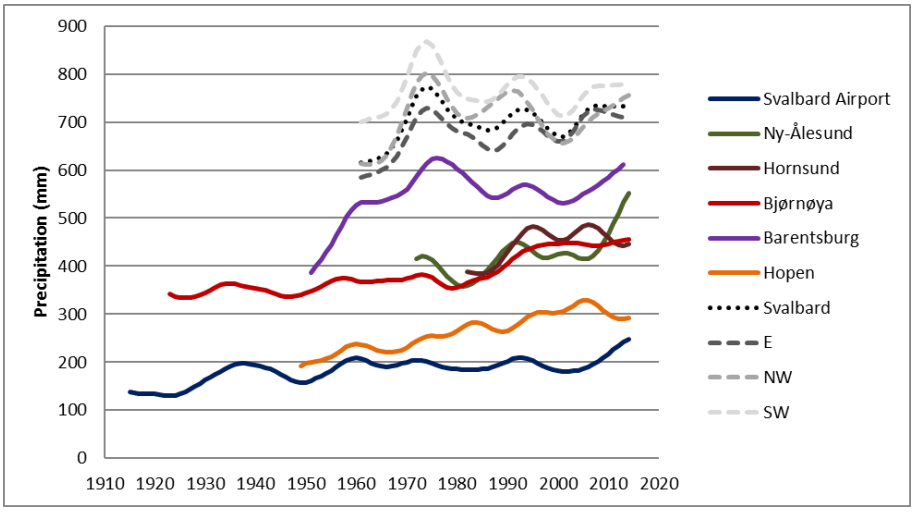

Figure 4.5 – Annual precipitation sum development at weather stations and for regions. Solid curves are based on homogenised observational series from weather stations, while the dotted curves are interpolated from the Sval-Imp data set. The low-pass filtered series are smoothed by Gaussian weighting coefficients, and show variability on a decadal time scale. The smoothed curves are cut three years from start and end.

region. The time series were extracted from the Sval-Imp data set at the grid cell covering the geographic location of the individual weather stations. For Svalbard Airport (Southwest), Hopen (East) and Ny-Ålesund (Northwest) the observed precipitation time series are shown as well. The region Southwest shows the largest variability between the stations but this is also the region with most stations.

The temporal development at all stations is very similar for the individual regions. For Southwest all the locations show maximum precipitation during the early 1970s, a secondary maximum during the early 1990s and a minimum of precipitation around 2000. Towards the end of the time series the precipitation increases again for all stations. In the eastern region a similar pattern in modelled precipitation can be detected for Kvitøya, Hopen, Edgeøya and Kongsøya. Karl XII Øya and Verlegenhuken, however, show a precipitation increase at the beginning of the time series (from around 1960 to 1970), a more or less constant trend afterwards and again a strong increase after 2000. The two station locations in the northwestern region exhibit the same pattern as the stations in the southwestern region, but the maximum in the early 1990s is more pronounced.

The observed precipitation at Hopen, Svalbard Airport and Ny-Ålesund is much lower than the precipitation from the Sval-Imp data set at the corresponding grid points. The main reason for the lower observed than modelled precipitation is undercatch in the precipitation gauges (see Section 4.6).

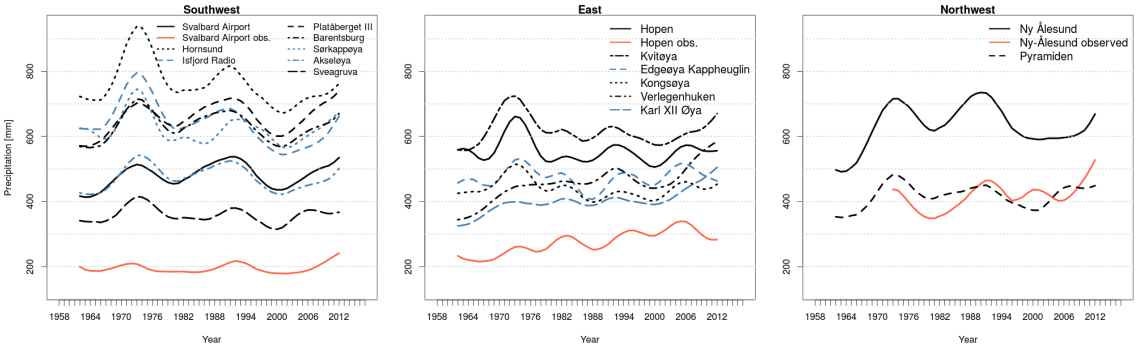

Figure 4.6 – Smoothed annual sums of precipitation for the grid points from Sval-Imp data set closest to the actual stations at the three Svalbard subregions and smoothed observed annual sums of selected stations for the years 1958-2017. The curves were filtered using a Gaussian filter such that variabilities smaller than 10 years were filtered out.

Though the observed precipitation shows the same temporal development as described above (maxima during the early 1970s and 1990s respectively and an increase after 2000) for two of the stations, namely Svalbard Airport and Ny Ålesund, the pattern is much less pronounced than for the Sval-Imp data set. At Hopen, the temporal development of the observed precipitation is different from the Sval-Imp data set.

4.4 Mean values for 30-year reference periods

Average annual and seasonal precipitation for Svalbard for the standard normal period $1961-1990$ and the reference period $1971-2000$ is presented in Table 4.1. The table includes values from measuring stations as well as for modelled values from the Sval-Imp data set. The Sval-Imp data set indicates average annual precipitation for Svalbard around 700 mm, with highest values for the southwestern region. The modelled precipitation is higher than the measured, but considering effects of gauge undercatch, the Sval-Imp data set in general seems to give a realistic picture of precipitation totals (see Section 4.6). The measured annual precipitation at Svalbard Airport is less than half of what is measured in Ny-Ålesund and Barentsburg, and also the Sval-Imp data set indicates values more than twice the amount measured at Svalbard Airport (Table 4.5).

At most stations the seasonal differences in measured precipitation are rather small, but in general the period May-June is the driest, and September-October the wettest (see Figure 4.3.1 in Hanssen-Bauer et al. (2019)). Except for Bjørnøya, all stations have a secondary precipitation maximum in March (Hanssen-Bauer et al.,

2019).

Table 4.2 shows the differences in annual precipitation between the "reference period" 1971-2000 and other 30-year periods (1961 – 1990, 1981 – 2010 and 1988 – 2017) both for measured values at weather stations as well as for regional values derived from the Sval-Imp data set. The Sval-Imp data shows small differences between the various periods, but a tendency to higher values for the reference period than present (1988 – 2017) because of the high modelled values in the 1970s. The measured precipitation - except for Barentsburg - indicates highest values for the most recent 30-year period. These features are in line with the graphs in Figure 4.5.

	1961-1990 average					1971-2000 average				
Station name	Ann	DJF	MAM	JJA	SON	Ann	DJF	MAM	JJA	SON
Bjørnøya	371	67	89	121	93	396	82	78	122	114
Hopen	250	47	41	84	77	276	58	55	83	79
Hornsund*	405	70	122	125	88	428	72	124	142	90
Isfjord Radio	480	99	121	140	120	NA	NA	NA	NA	NA
Barentsburg	565	127	93	173	173	581	134	100	175	172
Svalbard Airport	189	40	51	48	50	196	41	52	52	51
Ny-Ålesund	385	86	84	116	99	409	95	82	122	110
Svalbard total	694	143	162	224	164	723	153	164	225	181
Svalbard SW	770	162	163	245	197	791	172	167	240	213
Svalbard NW	714	155	173	214	171	745	165	181	219	181
Svalbard E	659	131	158	220	148	690	142	156	222	170

Table 4.1 – Annual and seasonal average precipitation [mm] for weather stations (observations) and for the three regions and entire Svalbard (from Sval-Imp data). *Start August 1978. Values for 1961-1990 from Førland (1993). Values for 1971-2000 based on 1978-2000.

Period	1961-1990	1981-2010	1988-2017
Bjørnøya	0.93	1.06	1.12
Hopen	0.91	1.08	1.08
Hornsund*	0.95	1.04	1.09
Barentsburg	0.97	0.95	0.97
Svalbard Airp	0.97	0.96	1.02
Ny-Ålesund	0.94	1.01	1.12
Svalbard SW	0.97	0.95	0.96
Svalbard NW	0.96	0.95	0.97
Svalbard East	0.96	0.99	1.00
Svalbard total	0.96	0.97	0.99

Table 4.2 – Ratios between annual precipitation for different 30-year periods and the reference period 1971-2000 for stations (observations) and regions (Sval-Imp data). *Hornsund: See legend for Table 4.1

	Svalbard	East	Northwest	Southwest
Annual	722.7	689.2	745	791.5
DJF	181.3	170.3	180.4	212.8
MAM	152.5	140.9	164.5	171.6
JJA	164.1	156.4	181.1	167
SON	224.8	221.6	219	240.2
JAN	64.7	61.8	62	75.6
FEB	53.2	48.1	56.7	63.8
MAR	61.8	55.6	66.5	73.8
APR	46	43.6	47.7	50.8
MAY	44.7	41.7	50.3	46.9
JUN	47.4	46.3	51	46.3
JUL	51.9	48.6	59.2	53.1
AUG	64.8	61.5	70.9	67.5
SEP	77.6	76.8	77.9	79.6
OCT	75.1	75.9	71.3	77.3
NOV	72.1	68.9	69.8	83.3
DEC	63.7	61.2	61.7	73.1

Table 4.3 – 30-year reference period (1971-2000). Annual, seasonal and monthly mean precipitation sum [mm] for subregions and entire Svalbard from the Sval-Imp data set.

	1961-1990 - 1971-2000				1981-2010 - 1971-2000				1988-2017 - 1971-2000			
	Svalbard	East	Northwest	Southwest	Sval	E	NW	SW	Sval	E	NW	SW
Annual	0.96	0.95	0.96	0.97	0.97	0.99	0.95	0.95	0.98	1.00	0.97	0.96
DJF	0.90	0.87	0.95	0.93	1.03	1.06	1.00	1.00	1.06	1.09	1.03	1.02
MAM	0.93	0.93	0.94	0.94	0.96	0.99	0.92	0.95	0.97	1.01	0.89	0.95
JJA	0.99	1.01	0.97	0.97	0.89	0.90	0.89	0.88	0.89	0.90	0.89	0.88
SON	0.99	0.99	1.02	1.02	0.98	0.99	0.98	0.96	1.00	1.00	1.04	0.99
JAN	0.84	0.80	0.87	0.87	1.05	1.06	1.05	1.03	1.07	1.06	1.11	1.07
FEB	0.93	0.91	0.95	0.95	1.01	1.06	0.94	0.96	1.03	1.10	0.95	0.97
MAR	0.90	0.90	0.92	0.92	0.92	0.96	0.88	0.89	0.95	1.02	0.85	0.91
APR	0.95	0.92	0.98	0.98	1.05	1.06	1.01	1.06	1.03	1.06	0.98	1.02
MAY	0.96	0.96	0.93	0.93	0.93	0.95	0.87	0.94	0.92	0.96	0.85	0.92
JUN	1.03	1.04	1.01	1.01	0.96	0.97	0.93	0.95	0.88	0.90	0.86	0.88
JUL	1.01	1.05	0.99	0.99	0.90	0.92	0.90	0.88	0.92	0.93	0.91	0.91
AUG	0.94	0.96	0.94	0.94	0.84	0.84	0.85	0.83	0.88	0.87	0.91	0.86
SEP	1.00	1.00	1.01	1.01	0.95	0.95	0.98	0.94	0.97	0.93	1.06	1.00
OCT	1.05	1.02	1.12	1.12	1.01	1.04	0.97	0.99	1.03	1.04	1.03	1.00
NOV	0.94	0.95	0.94	0.94	0.98	0.99	0.98	0.94	1.01	1.02	1.01	0.96
DEC	0.97	0.95	1.01	1.01	1.03	1.04	1.03	1.01	1.13	1.17	1.09	1.08

Table 4.4 – 30-year reference periods: Difference from 1961-1990, 1981-2010 and 1988-2017 respectively to the reference period 1971-2000. Annual, seasonal and monthly mean temperature for subregions and entire Svalbard from the Sval-Imp data set.

4.5 Covariation

Figure 4.7 summarises the correlations between the observed and the modelled precipitation (both from the CCLM and the Sval-Imp data set) for the different weather stations. To simplify the illustration only R^2 is shown. Note that different time periods were used for the Sval-Imp data and the CCLM model. The correlations are computed using the daily precipitation as well as the monthly means, for the whole year but also for the summer (Jun-Jul-Aug-Sep) and winter (Dec-Jan-Feb-Mar) months only. As can be seen, R^2 is considerably lower for precipitation than for temperature (see Fig. 3.7) and the variability of R^2 for precipitation is very high, the values reach from 0.1 to 0.9. The lowest R^2 can be found for Hornsund and Hopen, whereas Isfjord Radio and Ny-Ålesund have the highest values. The two different downscaling methods (see Sections 2.1 and 2.2) agree quite well for the different stations.

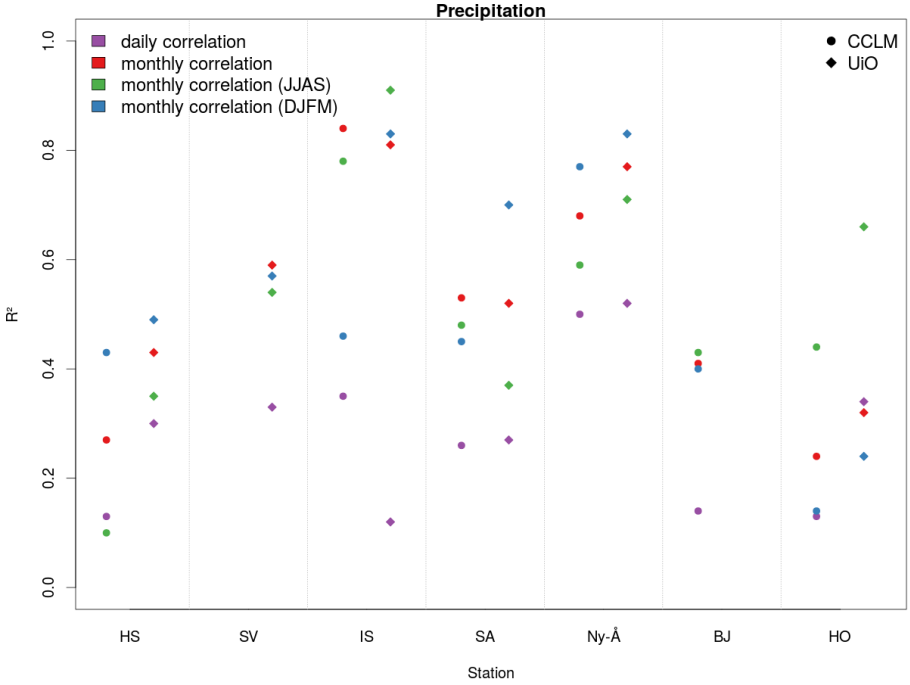

Figure 4.7 – R^2 for the different correlations between precipitation from observations and Sval-Imp and CCLM data, respectively. Note that the compared time periods are different for Sval-Imp and CCLM data. The abbreviations for the station names can be found in Table 2.1.

Some examples for these correlations can be found in Fig. 4.8, where the scatterplots for the daily observed and the daily Sval-Imp temperature are shown for four selected stations. As can be already seen in Fig. 4.7 the correlation for Ny-Ålesund

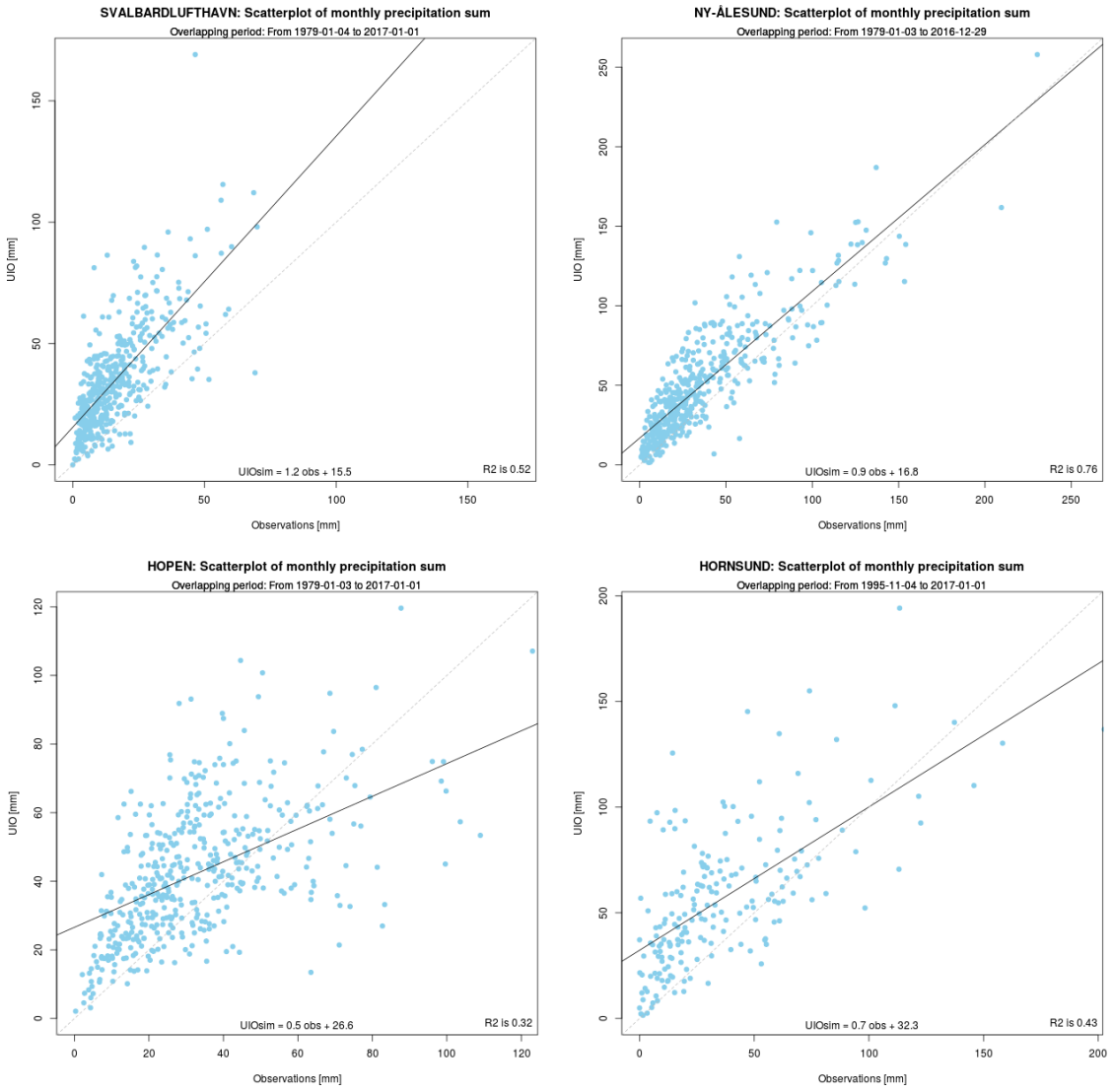

Figure 4.8 – Illustrated examples from Fig. 3.7: Scatterplots for precipitation from observations and Sval-Imp data. The lines indicate the regression line between Sval-Imp data and observations.

is better than the correlation for Svalbard Airport. However, at both stations the precipitation from the Sval-Imp data set overestimates the observed precipitation, especially the higher values at Svalbard Airport. The scatterplots for Hopen and Hornsund underline the low values of R^2 from Fig. 4.7. The observed precipitation is overestimated for the low precipitation values while it is underestimated for the high values for both stations.

4.6 Absolute values

Downscaled and observed annual and seasonal precipitation sums for Hopen, Svalbard Airport and Ny-Ålesund (Table 4.5) show that the values from the Sval-Imp data set are higher than the observed values for all stations and all seasons for the three time periods studied. The highest differences can be found for Hopen, where the modelled precipitation sums for winter and spring during the period $1961-1990$ are more than three times higher than observed.

Period	1961-1990			1971-2000			1988-2017		
	OBS	Sval-Imp	Ratio	OBS	Sval-Imp	Ratio	OBS	Sval-Imp	Ratio
ANNUAL									
Hopen	250	563	2.25	276	566	2.05	298	548	1.84
Svalbard Ap	189	471	2.49	196	492	2.51	200	501	2.51
Ny-Ålesund	385	630	1.64	409	668	1.63	459	653	1.42
SPRING									
Hopen	41	138	3.36	55	120	2.19	69	117	1.69
Svalbard Ap	40	111	2.78	41	107	2.61	32	100	3.07
Ny-Ålesund	86	156	1.81	95	155	1.64	87	128	1.48
SUMMER									
Hopen	84	120	1.43	83	121	1.46	70	112	1.59
Svalbard Ap	51	107	2.09	52	124	2.39	50	136	2.70
Ny-Ålesund	84	148	1.76	82	168	2.05	82	158	1.92
AUTUMN									
Hopen	77	143	1.86	79	172	2.17	87	182	2.10
Svalbard Ap	48	123	2,53	52	134	2.58	61	147	2.41
Ny-Ålesund	116	155	1.34	122	178	1.46	153	204	1.33
WINTER									
Hopen	47	162	3.44	58	153	2.64	71	137	1.93
Svalbard Ap	52	131	2.51	51	127	2.50	56	118	2.13
Ny-Ålesund	99	171	1.73	110	167	1.51	137	163	1.19

Table 4.5 – Seasonal and annual precipitation sums [mm] from observations (OBS) and the Sval-Imp data set (Sval-Imp). Ratio is Sval-Imp divided by OBS.

Except for Ny-Ålesund, the ratios between modelled and observed precipitation are largest during the spring season (Figure 4.9). One obvious reason for lower observed than modelled precipitation is the effect of undercatch in the precipitation gauges. In case of events with solid precipitation and strong winds, a large part of the precipitation is not "caught" by the gauges. Thus, the measured precipitation is just a small fraction of the "true precipitation" (Førland et al., 1996). In a study in Ny-Ålesund, Førland and Hanssen-Bauer (2000) found that because of undercatch, the "true" total precipitation during snowfall was almost twice the measured amount (see Section 4.8). Large undercatch for solid precipitation in

windy areas is confirmed by recent studies in mountainous areas (Haukeliseter) in the Norwegian mainland (Wolff et al., 2013, 2015).

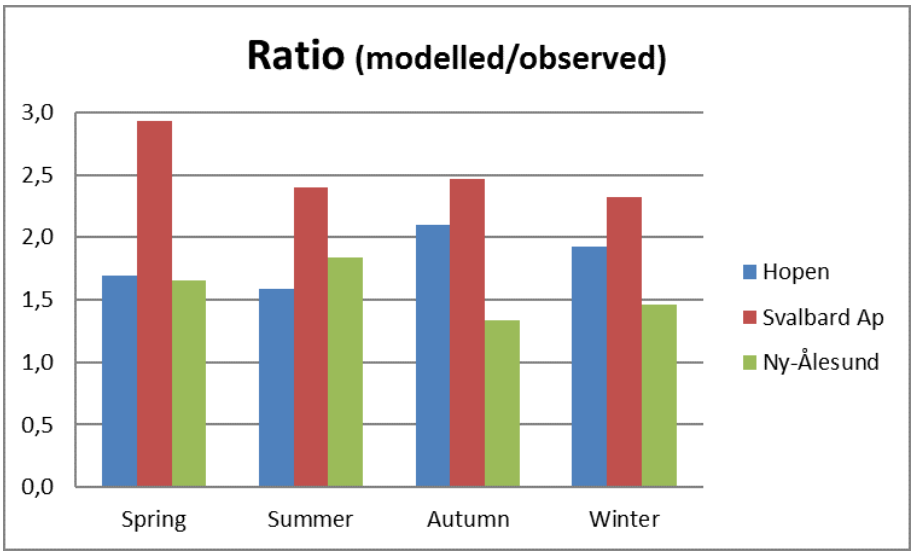

Figure 4.9 – Ratios between modelled (Sval-Imp data set) and observed precipitation. The ratios are averages for the results for the periods 1961-1990 and 1988-2017 presented in Table 4.5.

At Svalbard there may be snowfall events even in summer, and rain events (occasionally heavy rainfall) may occur even during mid-winter. With this mixture of snow and rain in all seasons, Førland and Hanssen-Bauer (2000) found the following seasonal average ratios between "true" and measured precipitation: Winter = 1.70, Spring = 1.55, Summer = 1.25 and Autumn = 1.45. For Ny-Ålesund - except for the summer season - the differences (ratios) in Table 4.5 between modelled and observed precipitation may be explained by undercatch. For Hopen the discrepancy between observed and modelled precipitation totals at the old measuring site could be explained by undercatch, but the observational values at the new site (cf. Section 2.3.2) are too low compared to the Sval-Imp totals.

For Svalbard Airport the discrepancies between modelled and observed precipitation are substantially higher than the undercatch ratios for all the seasons. However, the precipitation measured at Svalbard Airport is much lower than for the other stations at the western part of Spitsbergen. Table 4.5 shows that the annual precipitation at Ny-Ålesund is twice the amount of Svalbard Airport. In Barentsburg, just 34 km west of Svalbard Airport, the annual precipitation ($1971 - 2000$) is 581 mm (Table 4.1), i.e. nearly three times the value for Svalbard Airport. Thus, it seems as if the Longyearbyen area is situated in a "rain shadow" area, sheltered from precipitation by the surrounding mountains. Although the Sval-Imp data set

gives higher precipitation values for Ny-Ålesund than for Svalbard Airport, the topography resolved in the underlying model is probably not sufficient to reproduce the local "rain shadow" effect in the Longyearbyen area.

The main conclusion is hence that when considering undercatch effects, the Sval-Imp data set, except for Svalbard Airport, seems to give a realistic measure for precipitation totals. The Longyearbyen area is probably lying in a local "rain shadow" area, and a model with a higher resolution is needed to resolve the terrain details influencing the local precipitation in this area.

The time development of precipitation can be found in Table 4.6, studied by ratios between different 30-year time periods, i.e. respectively $1961-1990$ and $1988-2017$ versus the reference period $1971-2000$. For annual values the table demonstrates small differences between the various 30-year time periods for observations as well as modelled data. For Ny-Ålesund the observations indicate an increase of 12 % from $1971-2000$ to $1988-2017$, while the Sval-Imp data indicates reduced (2 %) annual precipitation. Also for Hopen, the measurements indicate increased annual precipitation while Sval-Imp gives a small decrease. Possible reasons for opposite trends in observed and modelled precipitation are discussed in Section 4.8.

	Ratio (%) 1961-1990 vs 1971-2000			Ratio (%) 1988-2017 vs 1971-2000		
	OBS	Sval-Imp	Diff	OBS	Sval-Imp	Diff
ANNUAL						
Hopen	91	99	8	108	97	-11
Svalbard Ap	96	96	0	102	102	0
Ny-Ålesund	94	94	0	112	98	-14
SPRING						
Hopen	75	115	40	126	97	-29
Svalbard Ap	97	103	6	79	93	14
Ny-Ålesund	91	100	9	92	82	-9
SUMMER						
Hopen	101	99	-2	85	92	7
Svalbard Ap	98	86	-12	97	109	13
Ny-Ålesund	102	88	-15	100	94	-6
AUTUMN						
Hopen	97	83	-14	110	106	-4
Svalbard Ap	94	92	-2	118	110	-8
Ny-Ålesund	95	87	-8	125	114	-11
WINTER						
Hopen	81	106	25	122	89	-33
Svalbard Ap	102	103	1	109	93	-16
Ny-Ålesund	90	103	13	124	98	-26

Table 4.6 – Seasonal and annual precipitation sums [mm] from observations (OBS) and Sval-Imp data set (Sval-Imp).

The seasonal differences do not give a consistent picture; positive and negative differences are found for most seasons and time periods. Whether the Sval-Imp data is able to reproduce the observed precipitation trends will be discussed further in Section 4.8.

4.7 Seasonal and monthly differences

To compare the Sval-Imp data and the CCLM simulations with the observations for single months and seasons, mean annual cycles of precipitation were computed. To summarise the results, Figure 4.10 shows the absolute biases between the mean annual cycles of precipitation from the Sval-Imp data and the CCLM model respectively and the observed precipitation. The biases for the single months were averaged over the whole year and over the four seasons to illustrate the differences.

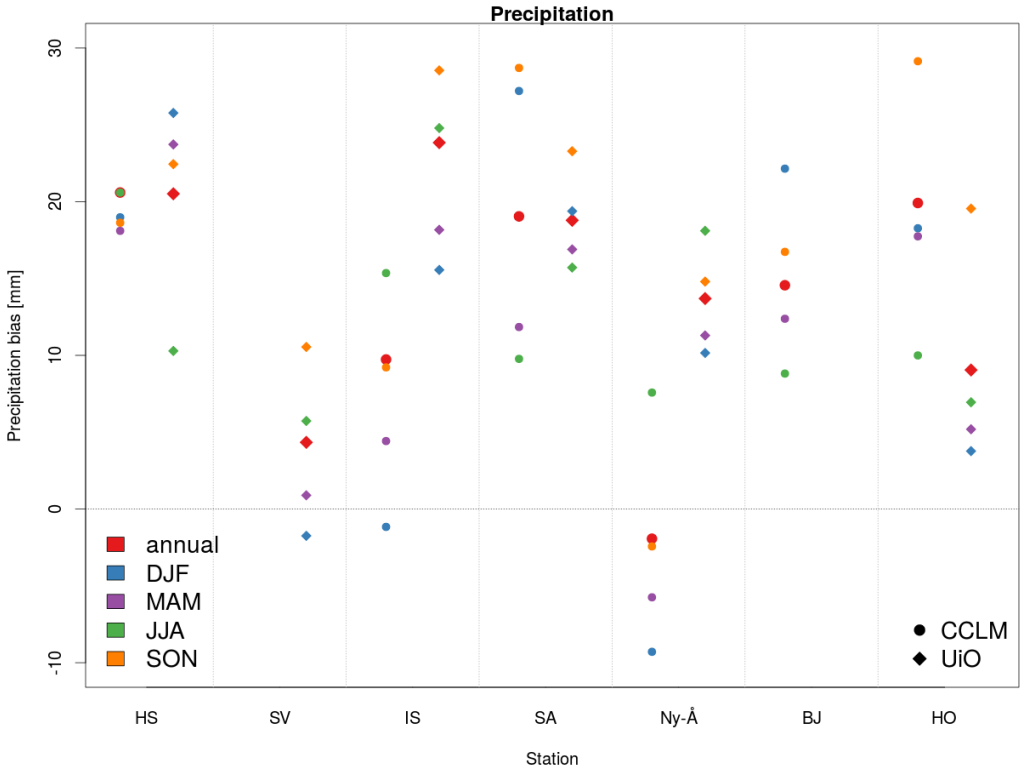

Figure 4.10 – Bias for the mean annual cycle of precipitation (in mm/month) from the CCLM simulations and the Sval-Imp data and the observations. For the annual bias all twelve months are considered, for the seasonal biases only the corresponding months are taken into account. The abbreviations for the station names are from Table 2.1.

In most cases the precipitation is overestimated by the models, this is in agreement to the results in previous sections. Only for Ny-Ålesund, the precipitation is underestimated by the CCLM model, except for the summer month. The precipitation from the Sval-Imp data set is considerably higher and overestimates the observed precipitation. Besides Ny-Ålesund, the two downscaling methods show different result for Isfjord Radio, the biases in this case are above 0 mm though.

Figure 4.11 shows the mean annual cycle for the Sval-Imp data set and the observations for Svalbard Airport and Ny-Ålesund. One can see that the precipitation is considerably higher for all months in the Sval-Imp data set (in agreement with Fig. 4.10). The difference is particularly high for the autumn months (SON) at Svalbard Airport and for the summer month (JJA) at Ny-Ålesund. The figure shows also that the modelled variability is considerably higher than the observed variability at Svalbard Airport, whereas it is also very high for observed precipitation at Ny-Ålesund.

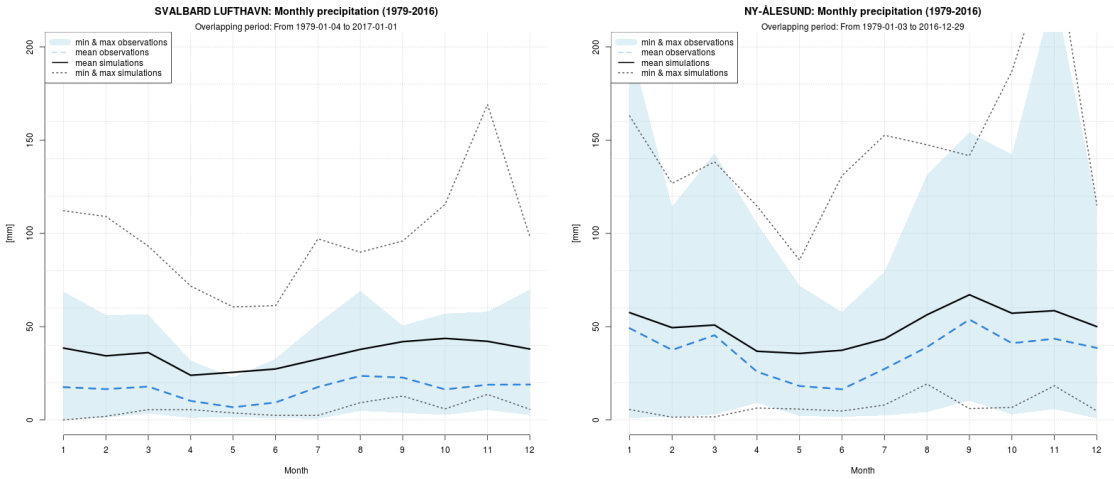

(a) Svalbard Airport **(b)** Ny Ålesund

Figure 4.11 – Monthly mean, minimum and maximum precipitation in mm from the Sval-Imp data (black) and the observations (blue) for Svalbard Airport and Ny Ålesund.

4.8 Linear trends

Linear precipitation trends for the Svalbard stations are outlined in Table 4.7. The left part presents trends from the start of the series, while the right part shows trends from 1971, the starting year for the reference period used in this report

and Hanssen-Bauer et al. (2019). For Svalbard Airport and Bjørnøya, the (statistical significant) centennial trends for annual precipitation show a linear increase of 3 % - 4 % per decade. For Svalbard Airport, the seasonal trends are highest for the autumn, while for Bjørnøya the increase is largest for winter and spring. For the latest fifty years (1971-present) only Bjørnøya, Hopen and Ny-Ålesund have significant (positive) trends for annual precipitation. Except for the shorter series from Hornsund, the largest seasonal increase (ca.15 % per decade) after 1971 is found for autumn at Svalbard Airport and Ny-Ålesund. For summer and spring there is a (non-significant) tendency of negative trends for all Spitsbergen stations.

		Start – 2017					1971 – 2017				
Station name	Start	Ann	DJF	MAM	JJA	SON	Ann	DJF	MAM	JJA	SON
Bjørnøya	1920	**3.2**	**4.9**	**5.2**	0.1	**2.3**	**6.4**	**12.1**	**11.7**	-4.7	4.3
Hopen*	1946	**6.8**	**12.2**	**13.2**	-0.1	**5.7**	**5.0**	**12.5**	**11.8**	-7.2	7.4
Hornsund**	1979	6.7	9.4	-5.7	-7.3	**23.6**	6.7	9.4	-5.7	-7.3	**23.6**
Barentsburg	1948	**3.9**	**3.7**	**4.3**	1.2	**5.6**	0.8	-2.3	-4.7	-6.6	6.6
Svalbard Ap	1912	**3.7**	2.4	2.7	**4.2**	**5.2**	4.1	8.4	-8.5	-1.2	**14.8**
Ny-Ålesund	1969	**7.8**	**13.3**	-0.4	-1.1	**15.2**	**7.1**	**14.4**	-3.3	-2.3	**15.5**
Svalbard total	1958	1.9	6.0	1.6	-1.3	1.7	-1.0	4.2	-2.5	-6.2	0.6
Svalbard SW	1958	0.5	3.2	1.0	-1.2	0.0	-2.3	1.8	-3.7	-7.1	0.0
Svalbard NW	1958	1.6	4.9	-0.2	0.1	2.7	-2.1	2.7	-6.2	-6.4	2.4
Svalbard E	1958	2.5	7.7	2.7	-2.1	1.9	0.0	5.8	-0.3	-5.8	0.1

Table 4.7 – Linear precipitation trends (% per decade relative to the 1971 − 2000 average) in the Svalbard region. The station values are computed from the observations while the region values are computed from the Sval-Imp data set. Trends significant at the 5 % level are bold. The statistical significance of trends was tested by the Mann-Kendall non-parametric test. Absolute trends in millimetres may be deduced by combining with the 1971 − 2000 averages in Table 4.3.

Table 4.7 shows that for the period 1971 − 2017 the measured annual precipitation has increased, while the downscaled reanalysis (Sval-Imp) indicate negative trends in this period. There may be several reasons for this discrepancy. The reanalysis data is not homogeneous during this period; e.g. ERA40 and ERAinterim were joined together in 1979 (see Section 2.3.2). The high modelled precipitation values in the 1970s (Figure 4.5) contribute to the negative trends in the Sval-Imp data set. The discrepancy may also be due to variations in large scale atmospheric circulation: while Sval-Imp covers large regions, all precipitation stations at Spitsbergen are situated on the western part. A small increase in westerly winds may increase orographic precipitation enhancement in the west, while a large part of Spitsbergen would be on the leeward side of the mountain ranges and would thus not be influenced by this enhancement.

However, there may also be another reason for this discrepancy: as mentioned in Section 4.6 there is a large undercatch in the precipitation gauges in the Arctic. This undercatch is larger for snow than for rain. In a study in Ny-Ålesund, Førland and Hanssen-Bauer (2000) found that to give a measure of "true" precipitation,

the average measured precipitation as snow should be adjusted by a factor of 1.85, and for rain by 1.15. Table 4.8 presents a simple exercise for Svalbard Airport and Ny-Ålesund to demonstrate that for the period 1971 − 2017 it is possible that the changes in measured precipitation are positive (4 % resp. 7 %) while the changes in "true precipitation" may be negative (−6 % resp. −1 %). As for Sval-Imp the trends in "true" precipitation are slightly negative, it is thus possible that while the measurements in the Svalbard region show increasing precipitation during 1971 − 2000, the "true" precipitation has decreased slightly. Most of the summer precipitation is falling as rain, and hence there is no significant contribution from shifting from solid to liquid precipitation in a warming climate. Accordingly, Table 4.7 shows that the trends for Jun-August are quite similar (and negative!) for Sval-Imp and measured precipitation.

	Longyearbyen	Ny-Ålesund
Annual precipitation in 1971 [mm] (see Table 4.1)	200	390
Linear trend 1971-2017 [%] (see Table 4.7)	4	7
Annual precipitation in 2017 [mm] linear trend	208	417
Snow/rain fraction in 1975 (see Figure 4.3.4 in Hanssen-Bauer et al. (2019))	50/50	38/62
Snow/rain fraction in 2017 (see Figure 4.3.4 in Hanssen-Bauer et al. (2019))	30/70	33/67
Rain/snow in 1971 [mm]	100/100	203/187
Rain/snow in 2017 [mm]	146/62	279/138
"True" precipitation in 1971 [mm]	100*1.15 + 100*1.85 = 300	203*1.15 + 187*1.85 = 579
"True" precipitation in 2017 [mm]	146*1.15 + 62*1.85 = 283	279*1.15 + 138*1.85 = 576
Change in measured precipitation 1971 to 2017	208/200 = 1.04	417/390 = 1.07
Change in "true" precipitation 1971 to 2017	283/300 = 0.94	576/579 = 0.99

Table 4.8 – Calculation example for demonstrating that changes in measured and "true" precipitation" may have opposite signs.

The conclusion is that time series corrected for undercatch should be used to study "real" precipitation trends in the Arctic. To correct the measured solid precipitation, the methodology developed by Wolff et al. (2013, 2015) could be applied on daily/hourly recordings of precipitation, temperature and wind at automatic weather stations. For manual measurements (daily/subdaily), alternatively the methodology described by Hanssen-Bauer et al. (1996) could be used to correct for undercatch.

5. Summary and conclusions

The network of weather stations observing temperature and precipitation in the Svalbard region is sparse. Most of the stations are located on the west coast, and at low altitudes. The biased location and limited number of stations is not sufficient to provide a representative description of temperature and precipitation over the entire Svalbard archipelago.

To provide a more consistent description of temperature and precipitation for the whole Svalbard area in the past, two reanalysis-based data sets are used in the main report about climate in Svalbard (Hanssen-Bauer et al., 2019) additionally to station measurements. This background report provides more detailed analysis of both data sets by comparing them to observations. The two reanalysis-based data sets are using different downscaling techniques to improve the spatial resolution. The Sval-Imp data set is developed and described in Østby et al. (2017) and uses both ERA40 and ERA Interim reanalysis. All variables are downscaled to 1 km x 1 km spatial resolution and have a temporal resolution of 6 h. The CCLM data set uses ERA Interim reanalysis as forcing to a dynamical regional climate model (the COSMO-CLM model), and ten variables are downscaled to 2.5 km x 2.5 km spatial resolution and have a temporal resolution of 1 h.

The Sval-Imp data set is used to produce maps of the long term mean of temperature and precipitation to get a picture of the spatial distribution of both variables. The spatial variation for temperature is rather similar for the different seasons: the highest temperatures are found in the southern and southwestern parts of the archipelago, while the lowest temperatures occur in mountainous and glacial areas in the north and east. The spatial distribution of precipitation shows the highest amounts in western mountain areas and lowest amounts in sheltered valleys and at low elevations in central and northeastern areas. This pattern is again similar for all seasons.

To perform time series statistics for the whole Svalbard area taking into account spatial variability, the area was divided in three regions. The Sval-Imp data set time series for temperature at the different regions show similar trends and decadal patterns as the the observed time series. However, the Sval-Imp data shows much lower temperatures because the Sval-Imp data, in contrast to weather stations,

covers higher altitudes and glacier-covered areas. The seasonal temperature time series for the Sval-Imp data set show that the highest increase occurs in winter, while the lowest increase occurs in summer. The seasonal precipitation time series are quite similar, the autumn precipitation being the highest in all three regions.

The general agreement between the observed and the modelled temperature (Sval-Imp data and CCLM simulation) is quite good, although there are examples like the station at Svalbard Airport, where the observed temperature is constantly higher than in the Sval-Imp data. The reason behind this could be the resolution of the Sval-Imp data: though it is quite high it still cannot resolve the actual geographical conditions. The low temperatures are often overestimated by the Sval-Imp data set whereas summer temperatures are often underestimated. The good agreement comes as no surprise as several of the Svalbard stations probably provided a basis for the reanalysis data which, in turn, was used to create the modelled data. The temperature trends show a good agreement as well. Thus, the Sval-Imp data set provides a very useful supplement to the observations, especially for the areas where no measurements are available.

The comparison between observed and modelled precipitation demonstrates that the modelled precipitation is much higher for all the stations. The main reason for this is undercatch in the precipitation gauges. This results in a considerably lower covariation between observed and modelled values. The difference between modelled and observed precipitation is especially high for Svalbard Airport. An explanation for this is the particular geographical position of the Longyearbyen area. The surrounding mountains shelter the area from precipitation, resulting in a "rain shadow" and thus lower observed precipitation. The resolution behind the Sval-Imp data set is not able to resolve this special circumstances. However, taking undercatch into account, the Sval-Imp data set seems to give a general realistic picture for precipitation.

Bibliography

ACIA. *Arctic Climate Impact Assessment*. Cambridge University Press, 2005. URL `http:/www.acia.uaf.edu`.

R. E. Benestad. What can present climate models tell us about climate change? *Climate Change*, 59(3):311–331, 2003.

L. Bengtsson, V. A. Semenov, and O. M. Johannessen. The early twentieth-century warming in the Arctic—A possible mechanism. *Journal of Climate*, 17(20):4045–4057, 2004.

A. Dobler, E. J. Førland, and K. Isaksen. Present and future heavy rainfall statistics for Svalbard - Background-report for Climate in Svalbard 2100. NCCS Report no. 3/2019, Norwegian Center of Climate Services, Oslo, Norway, 2019. URL `www.klimaservicesenter.no`.

E. J. Førland. Precipitation normals, Normal period 1961-1990. MET Norway KLIMA report 39, Norwegian Meteorological Institute, Oslo, Norway, 1993.

E. J. Førland and I. Hanssen-Bauer. Increased precipitation in the Norwegian Arctic: True or false? *Climatic Change*, 46:485–509, 2000. doi: 10.1023/A:1005613304674.

E. J. Førland, P. Allerup, B. Dahlström, E. Elomaa, T. Jónsson, H. Madsen, J. Perälä, P. Rissanen, H. Vedin, and F. Vejen. Manual for operational correction of nordic precipitation data. MET Norway report 24, Norwegian Meteorological Institute, Oslo, Norway, 1996.

E. J. Førland, I. Hanssen-Bauer, and Ø. Nordli. Climate statistics and long-term series of temperature and precipitation at Svalbard and Jan Mayen. MET Norway report 21, Norwegian Meteorological Institute, Oslo, Norway, 1997.

E. J. Førland, R. Benestad, I. Hanssen-Bauer, J. E. Haugen, and T. Engen-Skaugen. Temperature and precipitation development at Svalbard 1900-2100. *Advances in Meteorology*, 14(893790), 2011. doi: 10.1155/2011/893790.

B. Früh, A. Will, and C. L. Castro. Recent developments in Regional Climate Modelling with COSMO-CLM. *Meteorologische Zeitschrift*, 25(2):119–120, 2016.

H. M. Gjelten, Ø. Nordli, K. Isaksen, E. J. Førland, P. N. Sviashchennikov, P. Wyszynski, U. V. Prokhorova, R. Przybylak, B. V. Ivanov, and A. V. Urazgildeeva. Air temperature variations and gradients along the coast and fjords of western Spitsbergen. *Polar Research*, 35(1), 2016. doi: 10.3402/polar.v35.29878.

I. Hanssen-Bauer. Temperature and precipitation at Svalbard 1900-2050: Measurements and scenarios. *Polar Record*, 38:225–232, 2002.

I. Hanssen-Bauer and E. J. Førland. Long-term trends in temperature and precipitation in the Norwegian Arctic. Can they be explained by changes in the atmospheric circulation patterns? *Climate Research*, 10:143–153, 1998.

I. Hanssen-Bauer, E. J. Førland, and P. Ø. Nordli. Measured and true precipitation at Svalbard. MET Norway report 31/96, Norwegian Meteorological Institute, Oslo, Norway, 1996.

I. Hanssen-Bauer, E. J. Førland, H. Hisdal, S. Mayer, A. B. Sandø, and A. Sorteberg. Climate in Svalbard 2100. A knowledge base for climate adaptation. NCCS Report no. 1/2019, Norwegian Center of Climate Services, Oslo, Norway, 2019. URL `www.klimaservicesenter.no`.

K. Isaksen, E. Førland, A.Dobler, R.Benestad, J.E.Haugen, and A.Mezghani. Klimascenarier for Longyearbyen-området, Svalbard (In Norwegian). MET Norway Report 14, Norwegian Meteorological Institute, 2017.

E. Kessler. On the continuity and distribution of water substance in atmospheric circulations. *Atmospheric research*, 38(1-4):109–145, 1995.

S. Kotlarski, K. Keuler, O. B. Christensen, A. Colette, M. Déqué, A. Gobiet, K. Goergen, D. Jacob, D. Lüthi, E. Van Meijgaard, et al. Regional climate modeling on European scales: a joint standard evaluation of the EURO-CORDEX RCM ensemble. *Geoscientific Model Development*, 7(4):1297–1333, 2014.

O. Mestre, P. Domonkos, F. Picard, I. Auer, R. Böhm, E. Aguilar, J. Guijarro, G. Vertachnik, M. Klancar, B. Dubuisson, and P. Stepanek. Homer: a homogenisation software - methods and applications. *Idöjárás*, 117:47–67, 2013.

Ø. Nordli, I. Hanssen-Bauer, and E. J. Førland. Homogeneity analysis of temperature and precipitation series from Svalbard and Jan Mayen. MET Norway report 16, Norwegian Meteorological Institute, 1996.

Ø. Nordli, R. Przybylak, A. E. J. Ogilvie, and K. Isaksen. Long-term temperature trends and variability on Spitsbergen: The extended Svalbard Airport temperature series, 1898-2012. *Polar Research*, 33(21349), 2014. doi: 10.3402/polar.v33.21349.

T. I. Østby, T. V. Schuler, J. O. Hagen, R. Hock, J. Kohler, and C. H. Reijmer. Diagnosing the decline in climatic mass balance of glaciers in Svalbard over 1957–2014. *The Cryosphere*, 11(1):191–215, 2017. doi: 10.5194/tc-11-191-2017. URL `https://www.the-cryosphere.net/11/191/2017/`.

T. Peterson, D. Easterling, T. Karl, P. Groisman, N. Plummer, N. Nicholls, S. Torok, I. Auer, R. Boehm, D. Gullet, L. Vincent, H. R., H. Tuomenvirta, O. Mestre, T. Szentimrey, J. Salinger, E. Førland, I. Hanssen-Bauer, H. Alexandersson, P. Jones, and D. Parker. Homogeneity adjustments of in situ atmospheric climate data: a review. *International Journal of Climatatology*, 18:1493–1517, 1998.

I. V. Polyakov, R. V. Bekryaev, G. V. Alekseev, U. S. Bhatt, R. L. Colony, M. A. Johnson, A. P. Maskshtas, and D. Walsh. Variability and trends of air temperature and pressure in the maritime Arctic 1875-2000. *Journal of Climate*, 16:2067–2077, 2003.

A. F. Prein, W. Langhans, G. Fosser, A. Ferrone, N. Ban, K. Goergen, M. Keller, M. Tölle, O. Gutjahr, F. Feser, et al. A review on regional convection-permitting climate modeling: Demonstrations, prospects, and challenges. *Reviews of geophysics*, 53(2):323–361, 2015.

B. Ritter and J.-F. Geleyn. A comprehensive radiation scheme for numerical weather prediction models with potential applications in climate simulations. *Monthly Weather Review*, 120(2):303–325, 1992.

E. Schrodin and E. Heise. A New Multi-Layer Soil Model. Technical Report 2, COSMO Newsletter, 2002.

T. V. Schuler. Svalbard impact assessment forcing dataset, version 1 [data set]. Data set. Norstore. doi: 10.11582/2018.00006, 2018.

E. L. Steffensen. The climate at Norwegian Arctic stations. MET Report Klima 5, Norwegian Meteorological Institute, 1982.

E. L. Steffensen, P. Ø. Nordli, and I. Hanssen-Bauer. Stasjonshistorie for norske meteorologiske målinger i arktis. MET Report Klima 17/96, Norwegian Meteorological Institute, 1996.

SWIPA. *Snow, Water, Ice and Permafrost in the Arctic (SWIPA) 2017*. Arctic Monitoring and Assessment Programme (AMAP), Oslo, Norway, 2017.

M. Wolff, K. Isaksen, R. Brækkan, E. Alfnes, A. Petersen-Øverleir, and E. Ruud. Measurements of wind-induced loss of solid precipitation: description of a Norwegian field study. *Hydrology Research*, 44(1):35–43, 2013.

M. A. Wolff, K. Isaksen, A. Petersen-Øverleir, K. Ødemark, T. Reitan, and R. Brækkan. Derivation of a new continuous adjustment function for correcting wind-induced loss of solid precipitation: results of a Norwegian field study. *Hydrology and Earth System Sciences*, 19(2):951–967, 2015. doi: 10.5194/hess-19-951-2015. URL `https://www.hydrol-earth-syst-sci.net/19/951/2015/`.